Regulation of intracellular calcium and calcium buffering properties of rat isolated neurohypophysial nerve endings

Edward L. Stuenkel

Department of Physiology, University of Michigan, Ann Arbor, MI 48109, USA

1. Electrophysiological measurements of Ca^{2+} influx using patch clamp methodology were combined with fluorescent monitoring of the free intracellular calcium concentration ($[Ca^{2+}]_i$) to determine mechanisms of Ca^{2+} regulation in isolated nerve endings from the rat neurohypophysis.

2. Application of step depolarizations under voltage clamp resulted in voltage-dependent calcium influx (I_{Ca}) and increase in the $[Ca^{2+}]_i$. The increase in $[Ca^{2+}]_i$ was proportional to the time-integrated I_{Ca} for low calcium loads but approached an asymptote of $[Ca^{2+}]_i$ at large Ca^{2+} loads. These data indicate the presence of two distinct rapid Ca^{2+} buffering mechanisms.

3. Dialysis of fura-2, which competes for Ca^{2+} binding with the endogenous Ca^{2+} buffers, reduced the amplitude and increased the duration of the step depolarization-evoked Ca^{2+} transients. More than 99% of Ca^{2+} influx at low Ca^{2+} loads is immediately buffered by this endogenous buffer component, which probably consists of intracellular Ca^{2+} binding proteins.

4. The capacity of the endogenous buffer for binding Ca^{2+} remained stable during 300 s of dialysis of the nerve endings. These properties indicated that this Ca^{2+} buffer component was either immobile or of high molecular weight and slowly diffusible.

5. In the presence of large Ca^{2+} loads a second distinct Ca^{2+} buffer mechanism was resolved which limited increases in $[Ca^{2+}]_i$ to approximately 600 nM. This Ca^{2+} buffer exhibited high capacity but low affinity for Ca^{2+} and its presence resulted in a loss of proportionality between the integrated I_{Ca} and the increase in $[Ca^{2+}]_i$. This buffering mechanism was sensitive to the mitochondrial Ca^{2+} uptake inhibitor Ruthenium Red.

6. Basal $[Ca^{2+}]_i$, depolarization-induced changes in $[Ca^{2+}]_i$ and recovery of $[Ca^{2+}]_i$ to resting levels following an induced increase in $[Ca^{2+}]_i$ were unaffected by thapsigargin and cyclopiazonic acid, specific inhibitors of intracellular Ca^{2+}-ATPases. Caffeine and ryanodine were also without effect on Ca^{2+} regulation.

7. Evoked increases in $[Ca^{2+}]_i$, as well as rates of recovery from a Ca^{2+} load, were unaffected by the extracellular $[Na^+]$, suggesting a minimal role for Na^+–Ca^{2+} exchange in Ca^{2+} regulation in these nerve endings.

8. Application of repetitive step depolarizations for a constant period of stimulation resulted in a proportional frequency (up to 40 Hz)-dependent increase in $[Ca^{2+}]_i$. On the other hand, for a constant number of stimuli a reduction in the $[Ca^{2+}]_i$ increase per impulse was observed at higher frequencies. Application of step depolarizations, mimicking in duration and frequency those occurring during impulse bursting of a vasopressinergic neuron, raised $[Ca^{2+}]_i$ to values where, in addition to buffering by the endogenous cytoplasmic component, there occurred buffering by a Ruthenium Red-sensitive mechanism and by plasma membrane Ca^{2+}-ATPase activity.

9. It is suggested that the Ca^{2+} regulatory properties of the neurohypophysial nerve endings may, together with existing electrophysiological and secretory data on these nerve endings, explain the importance of phasic impulse bursting to potentiation of neuropeptide release from this system.

A number of diverse cellular functions are under strict regulation by the intracellular free calcium concentration ($[Ca^{2+}]_i$). For nerve terminals a change in the $[Ca^{2+}]_i$ is the critical event required to initiate the impulse-mediated exocytotic release of neurotransmitter or neurohormone (Augustine, Charlton & Smith, 1987). The strict reliance of neurotransmitter and neurohormone release on a change in $[Ca^{2+}]_i$ suggests that the mechanisms that operate to regulate the amplitude, shape and duration of the cytosolic calcium signal in nerve terminals are of great importance. These mechanisms can be grouped largely into those that mediate an increase in $[Ca^{2+}]_i$ and those that operate in a restorative fashion to reduce $[Ca^{2+}]_i$ to basal or resting conditions. Voltage-dependent calcium channels are primarily responsible for calcium influx that is associated with action potential invasion of the nerve ending (Katz & Miledi, 1967). Indeed, the relationship between calcium influx occurring through voltage-dependent calcium channels and the initiation of exocytotic secretion has been extensively investigated for nerve terminals in both vertebrate and invertebrate preparations (Llinas, Steinberg & Walton, 1976; Lindgren & Moore, 1991). Moreover, significant efforts have been made to characterize the specific voltage-dependent calcium channels involved in secretion and to elucidate mechanisms of their hormonal and second messenger regulation (Dayanithi *et al.* 1988; Obaid, Flores & Salzberg, 1989; Turner, Adams & Dunlap, 1992; Artalejo, Adams & Fox, 1994). While voltage-dependent calcium influx has been studied extensively, the involvement of additional mechanisms to increase $[Ca^{2+}]_i$ in nerve terminals including, potentially, mobilization of calcium from inositol 1,4,5-trisphosphate (IP_3), calcium-sensitive intracellular stores (e.g. calcium-induced calcium release) or secretory granules is less well understood. There have, however, been several reports demonstrating an increase in spontaneous and evoked neurotransmitter release at the neuromuscular junction in response to caffeine, thereby implicating a mechanism of calcium-induced calcium release (Onodera, 1973; Wilson, 1973).

Neurons possess a number of mechanisms to restore resting calcium levels and to very rapidly and efficiently buffer calcium challenges that occur to evoked calcium influx or possibly to intracellular calcium mobilization (Baker & McNaughton, 1976; Requena & Mullins, 1979; Ahmed & Conner, 1988). These homeostatic mechanisms can be generally categorized into (1) cytosolic or membrane delimited proteins which bind calcium, (2) ATP-dependent calcium pumps of the plasma membrane and of intracellular compartments, and (3) non-ATP-dependent calcium transporters, such as the electrogenic plasma membrane Na^+–Ca^{2+} exchanger and mitochondrial Ca^{2+} uptake. The presence of these mechanisms in nerve terminals has been well documented, although the relative contribution of each to calcium homeostasis is not clear and may vary considerably among nerve terminal types (Blaustein, Ratzlaff & Schweitzer, 1978*b*; Nordmann & Zyzek, 1982; Nachshen, 1985; Nicholls, 1989). Recently, calcium buffering characteristics in neuronal somata and in the neuroendocrine chromaffin cells have been re-examined at the single cell level using combined electrophysiological recording of evoked calcium currents simultaneously with optical monitoring of $[Ca^{2+}]_i$ (Thayer & Miller, 1990; Neher & Augustine, 1992). These studies have demonstrated that calcium entering during a step depolarization is rapidly buffered by high-capacity buffering mechanisms, and allow definition of the various buffering components at the single cell level. In spite of the critical importance of understanding calcium dynamics in nerve terminals similar studies have been difficult, especially at the level of single vertebrate nerve endings, largely as a result of size limitations and heterogeneity of terminal preparations. Therefore, the relationship between calcium influx and the cytoplasmic calcium buffers of nerve terminals is not well understood.

In the present study we have characterized the endogenous cytoplasmic buffer capacity of single nerve endings of the rat neurohypophysis and investigated the relative importance of Ca^{2+} homeostatic mechanisms. The studies use combined electrophysiological and optical approaches for evaluating Ca^{2+} regulation. We have observed that the neurosecretory nerve endings contain three distinct Ca^{2+} buffering mechanisms. One exhibits high-affinity, proportional Ca^{2+} binding, a second is a high-capacity buffering mechanism that becomes operative once a $[Ca^{2+}]_i$ set point is reached and a third is represented by energy-dependent Ca^{2+} efflux. No evidence for mobilization of Ca^{2+} from intracellular stores or of intracellular ATP-dependent Ca^{2+} uptake was found. We conclude by suggesting that the Ca^{2+} buffering characteristics of the nerve endings, when considered with previous electrophysiological and secretory data on these nerve endings, may explain the importance of phasic impulse bursting to potentiation of release of the neuropeptides oxytocin and vasopressin from this system. A portion of these results have appeared in abstract form (Stuenkel, 1993).

METHODS

Preparation of isolated nerve endings

Experiments were performed on isolated nerve endings of the neural lobe of the pituitary prepared from male Sprague–Dawley rats (225–325 g) as described previously (Cazalis, Dayanithi & Nordmann, 1987). The animals were killed by CO_2 asphyxiation, decapitated and the pituitary isolated. Following removal of the anterior lobe and the pars intermedia the neural lobe was very briefly homogenized in 100 μl of buffer containing (mM): sucrose, 270; EGTA, 2; Hepes, 10; with pH adjusted to 7·0 with Tris. The resulting

homogenate was directly aliquoted onto a glass coverslip forming the bottom of an open recording chamber. Following a 5 min period, during which the nerve endings settled and adhered to the chamber bottom, a continuous flow of physiological saline (1·5–2 ml min^{-1}) through the chamber was begun. The physiological saline solution (PSS) consisted of (mM): NaCl, 140; $KHCO_3$, 5; $MgCl_2$, 1; $CaCl_2$, 2·2; glucose, 10; and NaOH–Hepes; with pH adjusted to 7·2. The recording chamber was of elliptical shape, with a solution volume of 100 μl and included baffles on the influx and efflux ports to produce nearly laminar flow over the isolated nerve endings. The flow rate was sufficient to remove from the recording chamber, over a period of 20 min, non-adhered nerve endings, red blood cells and incompletely dissociated tissue resulting from the homogenization. Rapid change in the superfusion solution was accomplished through use of an 8-port distribution valve connected, at the chamber inflow, to a series of solution reservoirs. Measurements of chamber turnover by fluorescence spectroscopy showed that a 1000-fold change in probe concentration within the chamber was accomplished in 10 s. The isolated nerve endings adhering to the coverslip were spherical and primarily of small diameter ($\leqslant$2 μm), although a small number of nerve endings could routinely be found whose diameters were in the 6–12 μm range. It is these larger diameter isolated nerve endings upon which the experiments were performed. Identification of these structures as nerve endings is based on morphological (electron microscopy), immunocytochemical and physiological (arginine vasopressin secretion) evidence (Nordmann, Dayanithi & Lemos, 1987). They can easily be distinguished from the small number of pars intermedia cells retained in the preparation as the intermediate cells possess a nucleus and are generally of larger and more uniform diameter.

$[Ca^{2+}]_i$ measurements

Measurements of $[Ca^{2+}]_i$ were performed on single isolated nerve endings loaded with the fluorescent Ca^{2+} indicator fura-2 in a manner similar to that described previously (Stuenkel, 1990; Stuenkel & Nordmann, 1993*a*). In those experiments using simultaneous patch clamp electrophysiological measurements, fura-2 was loaded into the nerve ending by inclusion of fura-2 (potassium salt, 150 μM) in the pipette solution. In other experiments loading of the nerve endings with the indicator was accomplished by adding 1 μM of the acetoxymethyl ester of fura-2 (fura-2 AM) in dimethyl sulphoxide carrier (0·1% final concentration) to the PSS and flowing it over the nerve endings for a period of 20 min at 37 °C. The nerve endings were then rinsed with PSS for a period of 20 min before commencement of $[Ca^{2+}]_i$ monitoring. The cytosolic fura-2 concentration attained using this latter approach was estimated at 150 μM based on comparison of resulting fluorescence intensity with that occurring by direct fura-2 loading via the patch pipette. In both types of experiments the chamber was mounted on the stage of an inverted microscope (Nikon Diaphot) that was coupled to a photomultiplier-based AR-CM fluorescent system (SPEX Industries, Edison, NJ, USA). Single nerve endings were focused using a ×40 oil immersion epifluorescent objective (Nikon Fluor, NA 1·3) and optically masked from surrounding regions and from the recording patch pipette using a pinhole diaphragm. Nerve endings were illuminated with a 150 W xenon lamp, following passage through a digitally controlled chopper wheel, which in turn selected light that passed through 340, 365 or 380 nm excitation filters (full width half-maximum equal to 10 nm for 340 and 380 nm filters, 7 nm for 365 nm filter). Emitted light was passed through a 400 nm dichroic mirror and 500 $\pm$ 20 nm barrier filter and measured with a photon counting photomultiplier (R928, Hamamatsu, Bridgewater, NJ, USA). As the emitted signal associated with each excitation wavelength represents the averaged intensity collected over the entire nerve ending the measurements of $[Ca^{2+}]_i$ represent a spatially averaged value. Sampling rate varied with the specific experiment being performed. The maximum sample rate used integrated emitted photon counts at each wavelength over 3 ms and contained an excluded time of 3 ms, which resulted in a dual wavelength sample point each 9 ms.

Conversion of the ratios of emitted light from two excitation wavelengths to $[Ca^{2+}]_i$ was calculated according to the relationship given by Grynkiewicz, Poenie & Tsien (1985). The relationship is described by:

$$[Ca^{2+}]_i = K_{eff}((R - R_{min})/(R_{max} - R)), \quad (1)$$

where R_{min} and R_{max} represent the ratio of emitted light (for 340 and 380nm excitation) under Ca^{2+} limiting and saturating conditions, respectively. The constant K_{eff} (the effective dissociation constant of the indicator under our particular experimental conditions) was determined experimentally as described below and is not the same as the dissociation constant (K_d). Determination of the constants R_{min}, R_{max} and K_{eff} was performed using an *in vivo* method, as described previously by Neher (1989) and Augustine & Neher (1992), which loads fura-2 free acid and buffers directly into the cell using the whole-cell recording patch clamp configuration. The R_{max} value was obtained by dialysis of nerve endings with a pipette solution containing (mM): *N*-methyl-D-glucamine chloride (NMG-Cl), 140; $CaCl_2$, 2; fura-2, 0·15; Tris–Hepes, 40; with pH adjusted to 7·0. For the R_{min} pipette solution NMG-Cl was reduced to 130 mM, $CaCl_2$ was omitted and 10 mM Tris–EGTA added, but the solution was otherwise the same as the R_{max} solution. In addition to these solutions, nerve terminals were dialysed with a pipette solution buffered to contain a free calcium concentration of 0·34 μM using $CaCl_2$ (4·6 mM) and Tris–EGTA (10 mM). Intensity measurements (counts per second) of emitted light associated with each pair of excitation wavelengths (340 and 380 nm; and 365 and 380 nm) for each of the above pipette solutions were recorded and used to calculate the calibration constants. Calculation of the K_{eff} value was performed by substitution of the ratio values obtained for the 0·34 μM Ca^{2+} solution into the above relationship and using the R_{min} and R_{max} values for the appropriate excitation wavelengths. The R_{min}, R_{max} and K_{eff} values were 0·34, 11·0 and 5·4 μM (340 and 380 nm) and 0·64, 3·7 and 3·8 μM (365 and 380 nm), respectively. The *in vivo* method of fura-2 calibration was chosen to control for cytoplasmic viscosity, effects of membranous structures within the cytoplasm (e.g. secretory granules), path length, indicator concentration and background fluorescence of the fura-2-containing recording pipette. In all electrophysiological experiments the background fluorescence contributed by emitted light from fura-2 in the recording pipette was minimized by adjusting the focus below the plane of the recording pipette and by optically masking the region of the terminal on which the pipette made contact. Measurements of

background fluorescence made after formation of a gigaseal but prior to conversion to whole-cell recording showed that approximately 32% of the whole-cell fura-2 signal was attributable to this background.

Determination of endogenous buffer capacity of nerve endings

The capacity of a rapid cytoplasmic Ca^{2+} buffer (k_S) was determined for single nerve endings using the method described by Neher & Augustine (1992) on chromaffin cells. This method is based on a model where fura-2, dialysed into the cell via a patch pipette, will compete with fast endogenous cytoplasmic Ca^{2+} buffers for free cytoplasmic Ca^{2+}. The calculations account for the slower diffusion of Ca^{2+} and its buffers into and out of the patch pipette. The specific evaluation used in the present study is based on determining the amount of Ca^{2+} bound to fura-2. The evaluation requires the simultaneous measurement of evoked Ca^{2+} currents and changes in $[Ca^{2+}]_i$ as fura-2 dialyses into the cell following patch rupture and attainment of the whole-cell recording configuration. It also requires the determination of the fura-2 concentration at the time of the evoked change in $[Ca^{2+}]_i$, and thus for these experiments one of the excitation wavelengths was at the isostilbic point for fura-2 (365 nm) while the other was at a Ca^{2+}-sensitive wavelength (380 nm). The determination requires knowledge of the buffering characteristics of the exogenously introduced Ca^{2+} buffer, fura-2, in the cell. The calcium binding capacity of intracellular fura-2 (k_B) was calculated according to the equation given by Neher & Augustine (1992):

$$k_B = K_B[B_T]/(1 + [Ca^{2+}]_i K_B)^2, \quad (2)$$

where K_B represents the binding constant of intracellular fura-2 for calcium and B_T the cytoplasmic concentration of fura-2. K_B calculated from the fura-2 calibration data had a value of $1{\cdot}5 \times 10^6$ M^{-1}. The binding capacity of the endogenous cytoplasmic buffer (k_S; bound calcium over free calcium) can be related to the binding capacity of intracellular fura-2 according to the relationship:

$$k_S = k_B[(f_{max} - f)/f] - 1, \quad (3)$$

where f represents the amount of Ca^{2+} influx that binds to fura-2 and f_{max} the fraction of calcium bound at saturating fura-2 concentrations. The value is defined as:

$$f = \Delta F_{380}/\int I_{Ca} dt, \quad (4)$$

where ΔF_{380} is the change in emitted light intensity corresponding to the 380 nm excitation. The value of f_{max} was determined from the ordinate intercept of the double reciprocal plot of f *versus* k_B.

Electrophysiological recording

Conventional whole-cell patch clamp recording methods (Hamill, Marty, Neher, Sakmann & Sigworth, 1981) were used to evoke and record calcium currents from single nerve endings. Patch pipettes with resistances of 7–10 MΩ were constructed out of capillary glass (1·5 mm o.d., Drummond Scientific, Broomall, PA, USA), coated with Sylgard (Dow Corning, Midland, MI, USA) and fire polished. Following a 20–30 min period of continuous PSS superfusion, the extracellular buffer solution was changed to that in which current recordings were made consisting of (mM): tetraethylammonium chloride, 137; $CaCl_2$, 10; $MgCl_2$, 2; glucose, 19; Hepes, 10; with pH adjusted to 7·2 with Tris. In a number of experiments the $CaCl_2$ concentration was reduced to 1 or 2·2 mM, which was accompanied by an increase in TEA-Cl to maintain an osmolarity of 300–305 mosmol l^{-1}. The pipette solution contained (mM): NMG-Cl, 140; fura-2 (potassium salt), 0·15; Mg-ATP, 2; Tris-EGTA, 0·1; Hepes, 40; with pH adjusted to 7·0 and osmolarity adjusted to 295–300 mosmol l^{-1}. There are a number of experiments in which variations of the above pipette solution were used. For example, it should be noted that in experiments defining the endogenous Ca^{2+} buffer capacity no Tris–EGTA was included in the pipette and the fura-2 concentration was increased to 400 or 800 μM as indicated. The ionic composition of the bath and pipette solutions were designed to isolate voltage-dependent Ca^{2+} currents (I_{Ca}) from other voltage-sensitive currents present in these nerve endings (e.g. K^+, Na^+). In those experiments where the effects of voltage-dependent Na^+ currents on Ca^{2+} dynamics were examined, NaCl was substituted on an equal osmolar basis for NMG-Cl. Currents were recorded at room temperature (20–25 °C) using an Axon Instruments (Burlingame, CA, USA) Axopatch-1D patch clamp amplifier. Pulse protocols, data acquisition and analyses were performed using pCLAMP software (Axon Instruments). Currents were filtered at 5 or 10 kHz (−3 dB) through a 4-pole Bessel filter, prior to digitization. Electrode capacitance was compensated electronically before transition to whole-cell recording. Corrections for linear leak currents and in some records for capacity transients were performed either off-line through averaging and scaling of applied hyperpolarizing pulses or through the use of an on-line P/N pulse protocol. Maintenance of stable and low basal $[Ca^{2+}]_i$ values in the patch-clamped nerve terminals required high resistance seals (> 10 GΩ) and very low steady leakage current. Recordings were terminated when the steady leak current exceeded 10 pA. Based on the time required for recovery of basal $[Ca^{2+}]_i$ following an evoked I_{Ca}, interpulse intervals were generally of 30–45 s duration. The exception to this protocol is the series of experiments where frequency-dependent changes in I_{Ca} and $[Ca^{2+}]_i$ were studied. In those experiments the step depolarizations were driven by gating the Axopatch-1D command voltage externally. In all experiments, at least 30 s was allowed after changes in holding potential before applying step depolarizations.

There exist a number of limitations of the methodological strategies used here for defining nerve terminal Ca^{2+} buffers. Use of the whole-cell recording configuration can rapidly dialyse diffusible Ca^{2+} buffers or, as a result of the pipette solution used, alter the properties of those Ca^{2+} buffers that remain (Zhou & Neher, 1993). In addition, the introduced fura-2 can have very significant effects on measurements of the amplitude and time course of evoked changes in $[Ca^{2+}]_i$ and on the endogenous Ca^{2+} binding capacity. The calculated $[Ca^{2+}]_i$ values also depend upon accurate determination of the calibration constants under identical recording conditions. Moreover, as a result of limited temporal and spatial resolution, the measurements of averaged cytosolic $[Ca^{2+}]_i$ calculated are likely to greatly underestimate the steep Ca^{2+} gradients established near the plasma membrane.

RESULTS

Activation of I_{Ca} and increase in $[Ca^{2+}]_i$ in isolated nerve endings

Figure 1 illustrates the effects of a brief step depolarization from −90 to +10 mV to elicit an inward current and induce a transient change in $[Ca^{2+}]_i$. The inward current shown was recorded in the presence of 10 mM external Ca^{2+}

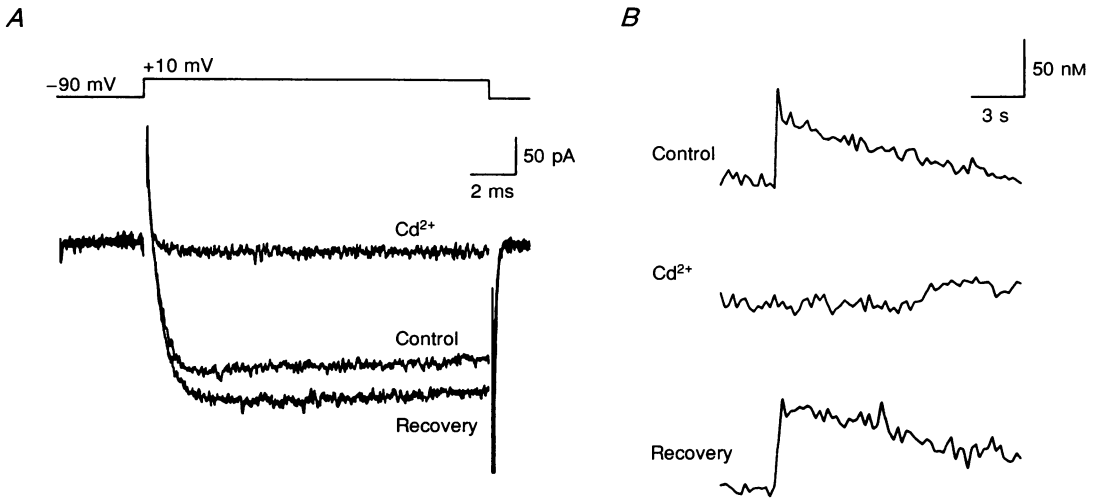

Figure 1. Relationship of depolarization-evoked calcium currents to $[Ca^{2+}]_i$
I_{Ca} (*A*) and corresponding change in $[Ca^{2+}]_i$ (*B*) evoked in response to 15 ms step depolarizing pulses to +10 mV (holding potential (V_h) = −90 mV). Both the I_{Ca} and the increase in $[Ca^{2+}]_i$ are reversibly blocked by 100 μM Cd^{2+} in the bath solution. I_{Ca} shown were not leak subtracted.

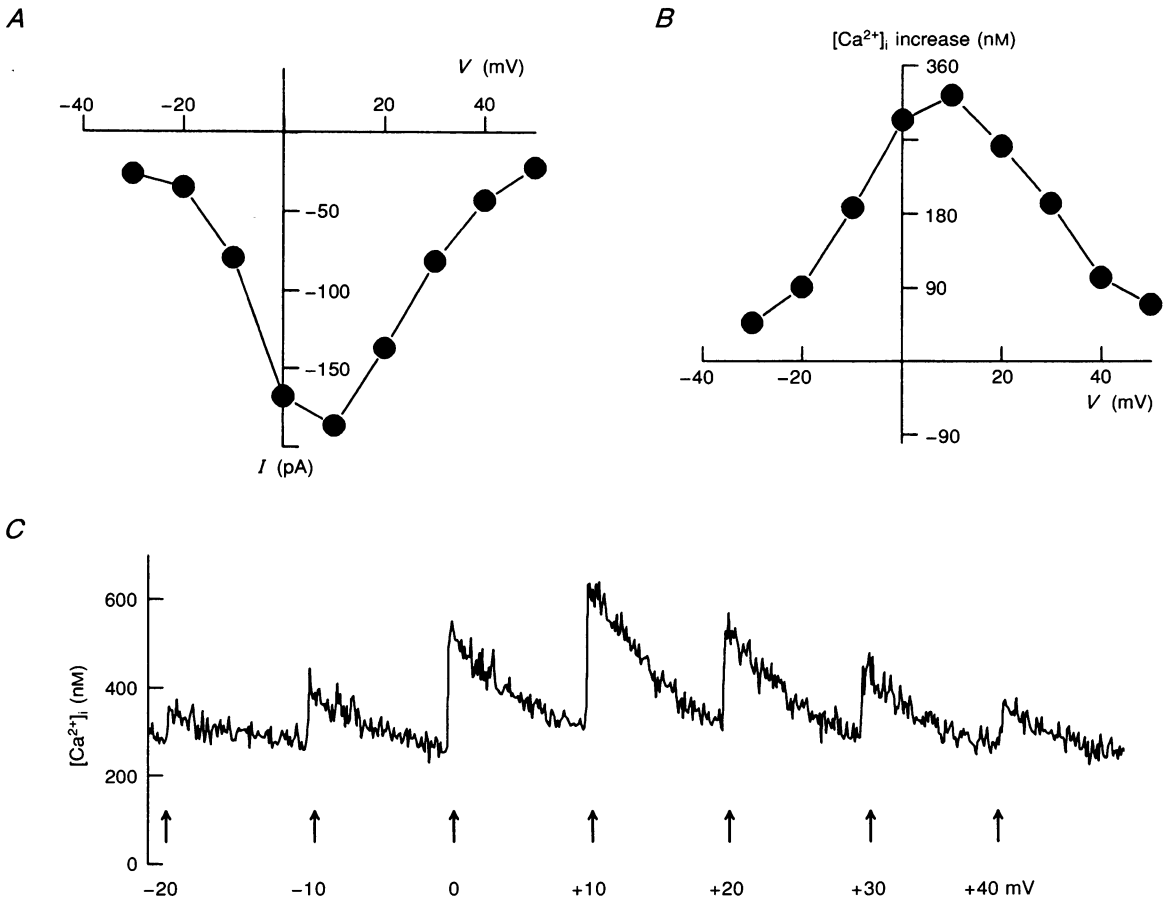

Figure 2. Relationship of I_{Ca} and $[Ca^{2+}]_i$ *versus* voltage for a single nerve ending
Comparison of the current–voltage relation for I_{Ca} (*A*; V_h = −90 mV) and corresponding increase in $[Ca^{2+}]_i$ (*B*). *C*, recording of $[Ca^{2+}]_i$ responses in this nerve ending to sequentially applied step depolarizations (67 ms step duration, 20 s interpulse interval). I_{Ca} values were obtained following linear and capacitative leak subtraction.

and peaked at approximately 150 pA within 1·2 ms of the applied step depolarization. Under the recording conditions used, the inward current is nearly completely represented by inward Ca^{2+} current through voltage- sensitive Ca^{2+} channels. This is evidenced by complete block of the evoked current in the presence of 100 μM Cd^{2+} added to the external medium and recovery of the inward current on removal of the Cd^{2+} (Fig. 1*A*). Inward currents evoked under similar ionic conditions were also sensitive to reduction or elevation of the external calcium concentration in a manner consistent with the current being carried by Ca^{2+} ions (see Fig. 3). In addition, applied membrane depolarizations to +60 or +80 mV from −90 mV holding potentials resulted in no measurable inward current and little or no increase in $[Ca^{2+}]_i$. Application of brief step depolarizations transiently increased $[Ca^{2+}]_i$ in a manner consistent with the evoked currents (Fig. 1*B*). Thus, a change in $[Ca^{2+}]_i$ of approximately 80 nM was observed in the absence but not in the presence of external Cd^{2+} in the nerve ending shown. Note that in the records shown there was a slightly greater amplitude of the I_{Ca} over the control current on washout of Cd^{2+} and this resulted in a slightly larger and more sustained change in $[Ca^{2+}]_i$.

Figure 2 shows a current–voltage relationship for I_{Ca} and the corresponding change in $[Ca^{2+}]_i$ obtained from a single nerve terminal voltage clamped to a holding potential of −90 mV and stepped in series to potentials from −30 to +50 mV. The amplitude of the peak I_{Ca} reached a maximum at +10 mV and a sustained inward current was first detected on steps to about −30 mV. The peak I_{Ca} on steps to +10 mV from a −90 mV holding potential was −242 ± 14·7 pA (mean ± S.E.M.; $n = 72$) for nerve endings of mean diameter 8·4 ± 0·2 μm. The amplitude of the resulting increases in intracellular calcium closely paralleled the current–voltage relationship with the greatest increase occurring on steps to +10 mV. The increase in $[Ca^{2+}]_i$ in response to depolarizing pulses to +10 mV for 300 ms from a −90 mV holding potential averaged 312·5 ± 34 nM above the resting level of 260 ± 14 nM (means ± S.E.M.; $n = 30$). The above strict

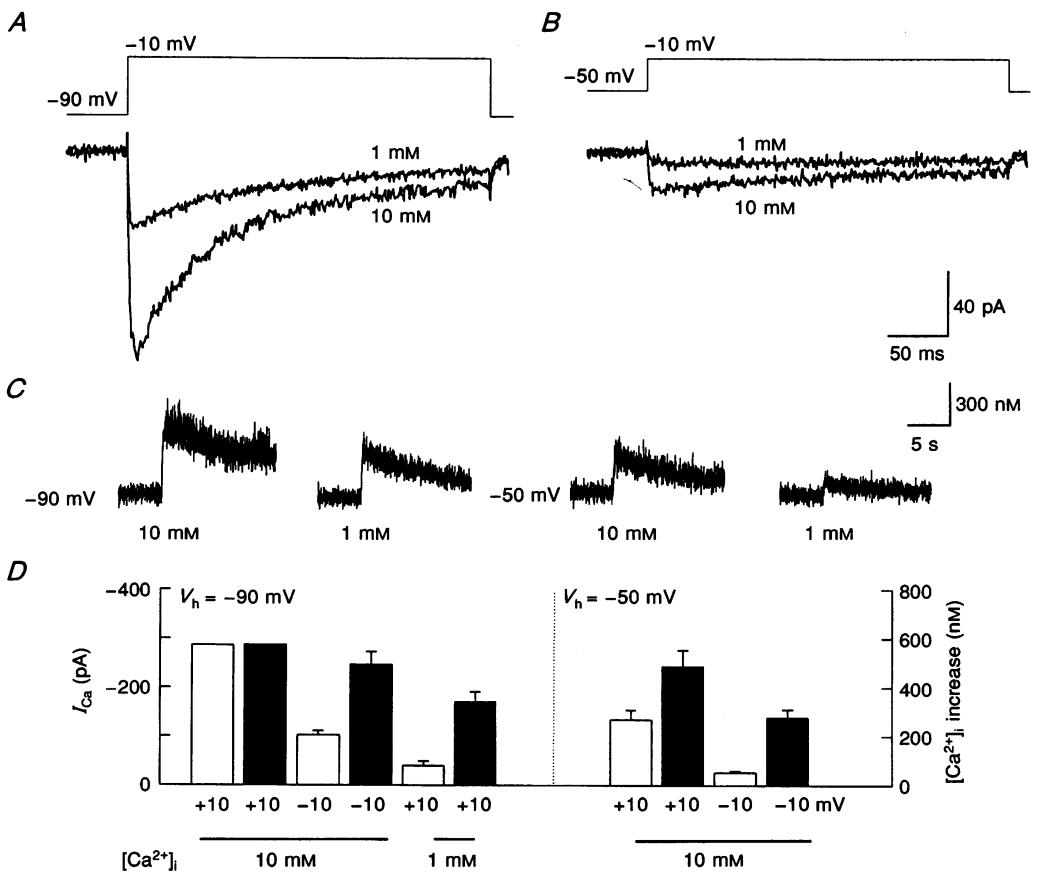

Figure 3. Effects of step depolarizations from different membrane holding potentials and $[Ca^{2+}]_o$ on I_{Ca} and $[Ca^{2+}]_i$

Comparison of step depolarizations to −10 from −90 (*A*) and −50 mV (*B*) holding potentials on I_{Ca} (*A* and *B*) and $[Ca^{2+}]_i$ (*C*) in the presence of 10 or 1 mM external calcium. All records shown are taken from a single nerve ending. *D*, comparison of averaged values from a number of similarly tested nerve endings. Open bins, I_{Ca}; filled bins, $[Ca^{2+}]_i$. Potential to which step depolarization was made is indicated under bars along with external $[Ca^{2+}]$.

correlation between the I_{Ca} and the increase in $[Ca^{2+}]_i$ suggests an apparent lack of voltage alone, or of Ca^{2+} influx, to mobilize intracellularly stored calcium in these nerve endings. The high value of the resting $[Ca^{2+}]_i$, relative to that reported for numerous other cell types, is likely to have resulted from the elevated extracellular Ca^{2+} concentration (10 mM) used. To test this possibility, a series of experiments examined the relationship of $[Ca^{2+}]_i$ to $[Ca^{2+}]_o$ in the nerve endings, while in the whole-cell recording configuration of the patch clamp. These experiments showed that resting $[Ca^{2+}]_i$ decreased from 248 ± 36 nM to 145 ± 22 nM (means ± S.E.M.; $n = 8$) on a 10-fold reduction in the extracellular $[Ca^{2+}]$ from 10 to 1 mM, respectively. We have reported previously on a similar dependence of $[Ca^{2+}]_i$ on $[Ca^{2+}]_o$ in intact, dissociated nerve endings of this preparation (Stuenkel & Nordmann, 1993*a*).

Relationship of $[Ca^{2+}]_o$ to Ca^{2+} influx

To characterize Ca^{2+} buffering properties in nerve endings a series of studies examined the relationship of the increase in $[Ca^{2+}]_i$ to depolarization evoked Ca^{2+} influx. Figure 3 shows representative data comparing I_{Ca} and changes in $[Ca^{2+}]_i$ in the presence of 10 or 1 mM external Ca^{2+} on step depolarizations to −10 from −90 (Fig. 3*A*) or −50 mV (Fig. 3*B*) holding potentials from a single nerve ending. The $[Ca^{2+}]_i$ in these experiments was sampled at the maximal rate, giving a ratio point each 9 ms. A rapidly decaying, transient I_{Ca} component, resulting presumably from activation and inactivation of N_t calcium channels (Lemos & Nowycky, 1989), was observed on steps from a holding potential of −90 mV and was absent on steps made from −50 mV holding potentials. Depolarizing steps to −10 mV from holding potentials of −50 mV predominantly activated high voltage-activated 'L-type' Ca^{2+} channels, as based on a previous report (Lemos & Nowycky, 1990). In spite of differences in the channel types activated and in the magnitude of the Ca^{2+} loads induced, the increase in $[Ca^{2+}]_i$ was found to correlate closely to the amplitude of the peak I_{Ca}. Figure 3*D* shows averaged data relating the amplitude of evoked peak currents to the change in $[Ca^{2+}]_i$ from the two holding potentials. The peak I_{Ca} on steps to +10 mV from a holding potential of −90 mV at 10 and 1 mM external $[Ca^{2+}]$ averaged −286·3 ± 57·4 and −39·7 ± 9·2 pA (means ± S.E.M.; $n = 4$), respectively. In comparison, steps to +10 mV from a holding potential of −50 mV measured in these same nerve endings gave a peak I_{Ca} of −143·3 ± 30·2 pA in 10 mM $[Ca^{2+}]_o$. The induced increases in $[Ca^{2+}]_i$ closely followed the amplitude of the evoked peak I_{Ca} (Fig. 3*C*). The rate of increase in $[Ca^{2+}]_i$ was, however, slower for step depolarizations from −50 than from −90 mV. In addition, initiation of a decline towards basal $[Ca^{2+}]_i$ following the step depolarization was delayed in the presence of 10 mM $[Ca^{2+}]_o$ with respect to the response at 1 mM.

A further comparison of evoked increases in $[Ca^{2+}]_i$ at 10 and 1 mM external Ca^{2+} is shown in Fig. 4. Figure 4*A* plots the increase in $[Ca^{2+}]_i$ against the duration of an applied step depolarization to +10 mV from a −90 mV holding potential. The data indicate that there is approximately a 10-fold difference in the duration of the step depolarization required to achieve a given change in $[Ca^{2+}]_i$ at 10 *versus* 1 mM external calcium. Increasing Ca^{2+} influx by elevating $[Ca^{2+}]_o$ to 10 from 1 mM, while requiring shorter pulse durations to produce a given increase in $[Ca^{2+}]_i$, did not shift the relation between the increase in $[Ca^{2+}]_i$ and Ca^{2+}

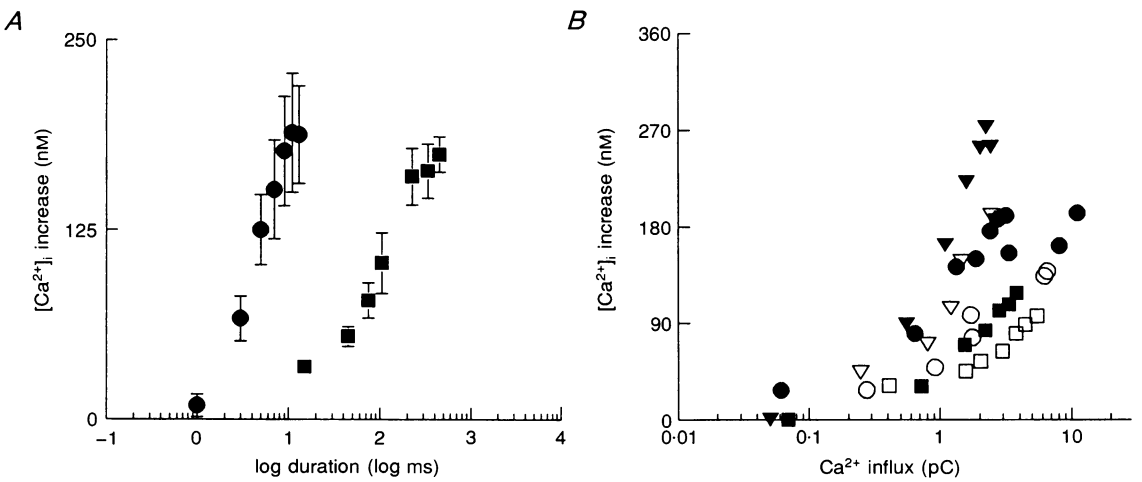

Figure 4. Comparison of pulse step duration and of time integrated calcium influx to the induced increase in $[Ca^{2+}]_i$

A, effect of duration of applied step depolarization (−90 mV holding potential, +10 mV step potential) on $[Ca^{2+}]_i$ increase at 1 (■) and 10 mM external calcium (●). *B*, comparison of calcium influx *versus* $[Ca^{2+}]_i$ increase for nerve endings in 1 mM (filled symbols, $n = 3$) or 10 mM (open symbols; $n = 3$) external calcium (−90 mV holding potential, +10 mV step potential). Each symbol type represents measurements from a different nerve ending.

influx (Fig. 4*B*). Thus, alterations in the $[Ca^{2+}]_o$ provide an unbiased method by which to alter stimulus evoked cytoplasmic Ca^{2+} loads.

A comparison of the time integral of the I_{Ca} to the net increase in $[Ca^{2+}]_i$ *during* the applied step depolarization is shown in Fig. 5. Various calcium loads were given by varying the holding potential, step potential (−10 or +10 mV) or $[Ca^{2+}]_o$. The data are taken from the experiments shown in Fig. 3*A* and *B*. The relationship was found to be nearly linear for smaller calcium loads (Fig. 5*A–C*) but became non-linear as the Ca^{2+} load was increased. The increase in $[Ca^{2+}]_i$ in response to large Ca^{2+} currents reached a characteristic plateau (Fig. 5*D*). The increase in $[Ca^{2+}]_i$ at which the plateau occurred, as measured over a number of different nerve endings, averaged 587·3 ± 15·7 nM (mean ± S.E.M.; $n = 8$). Figure 6 illustrates the individualized data obtained from these nerve endings at three time points during the applied 300 ms step depolarization. Time integrated currents exceeding approximately 10 pC resulted in a change in $[Ca^{2+}]_i$ that was no longer proportional to the Ca^{2+} influx. For nearly all the nerve endings, even under conditions optimal for inducing large calcium loads, this magnitude of an integrated current required approximately 50 ms of depolarization. Notably, for integrated currents as large as 30–40 pC the change in $[Ca^{2+}]_i$ was found not to exceed the approximately 600 nM seen associated with integrated currents of 10–15 pC, thereby suggesting an efficient Ca^{2+} buffer of high capacity. Figure 7 shows that

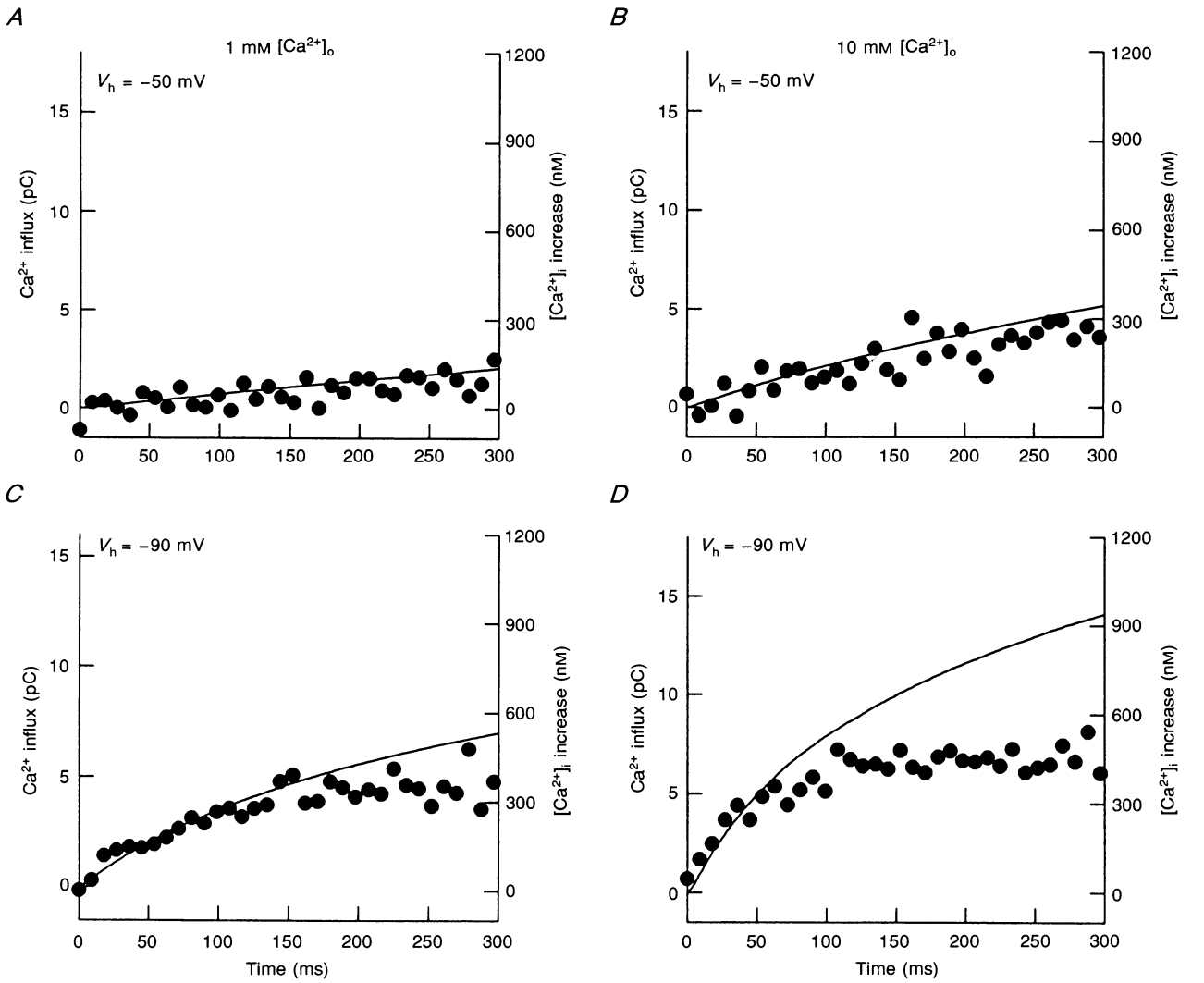

Figure 5. Relationship of Ca^{2+} influx to change in $[Ca^{2+}]_i$ as measured during step depolarizations

Step depolarizations were of 300 ms duration with steps to −10 mV from a holding potential of −50 (*A* and *B*) or −90 mV (*C* and *D*); external Ca^{2+} was 1 (*A* and *C*) or 10 mM (*B* and *D*). A $[Ca^{2+}]_i$ determination (●) was made each 9 ms while I_{Ca} (continuous line) was simultaneously recorded. Data shown is from a single nerve ending and is representative of data obtained from 11 such experiments.

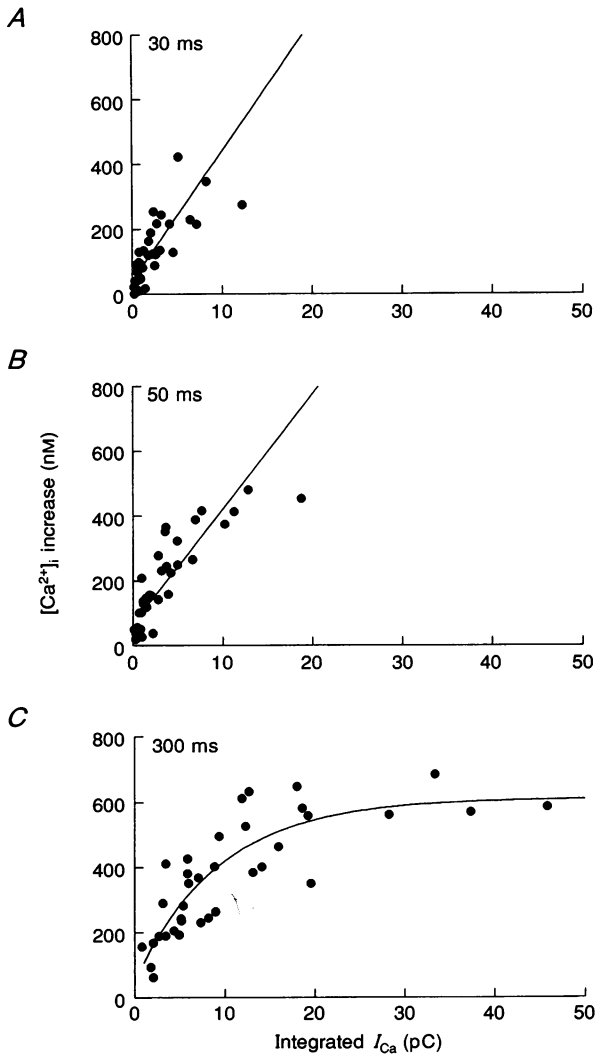

Figure 6. Comparison of Ca^{2+} influx–$[Ca^{2+}]_i$ relationship at intervals during a step depolarization
The relationships were formed from values taken at 30, 50 and 300 ms (top to bottom) time points during step depolarizations. Alteration of external $[Ca^{2+}]$ or of holding potential provided a range of Ca^{2+} loads such as those shown in Fig. 5. Data shown were obtained from measurements on 11 separate nerve endings. Lines represent a linear regression (*A* and *B*) or single exponential (*C*) fit of data points.

application of step depolarizations in close temporal sequence (2 sec interval) which failed to induce facilitation of the $[Ca^{2+}]_i$ increase and indeed resulted in only a nominal change in $[Ca^{2+}]_i$. These data also suggest the presence of efficient cytoplasmic calcium buffering when $[Ca^{2+}]_i$ reaches a given value.

To investigate if the buffering of free calcium in the presence of large calcium loads could result from mitochondrial Ca^{2+} uptake, a series of experiments were performed using Ruthenium Red (10 μM; included in the recording pipette), which is known to block mitochondrial Ca^{2+} uptake (Moore, 1971). Figure 8

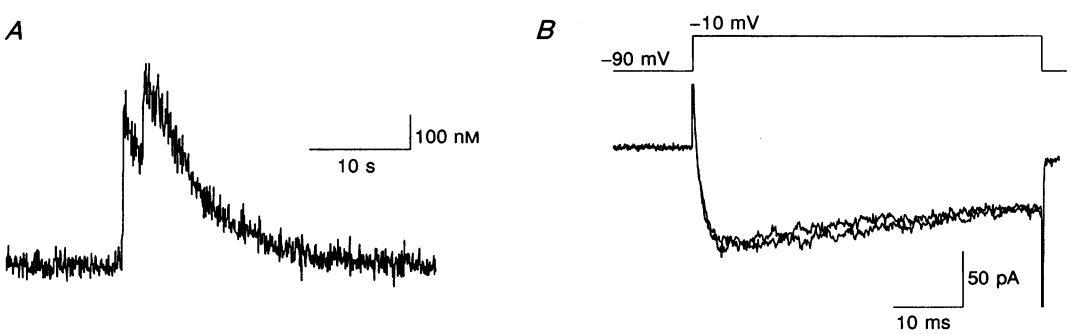

Figure 7. Effect of step depolarizations applied in close temporal sequence on $[Ca^{2+}]_i$ (*A*) and I_{Ca} (*B*)
Step depolarizations to −10 mV were applied from a holding potential of −90 mV. The interpulse duration was 2 s.

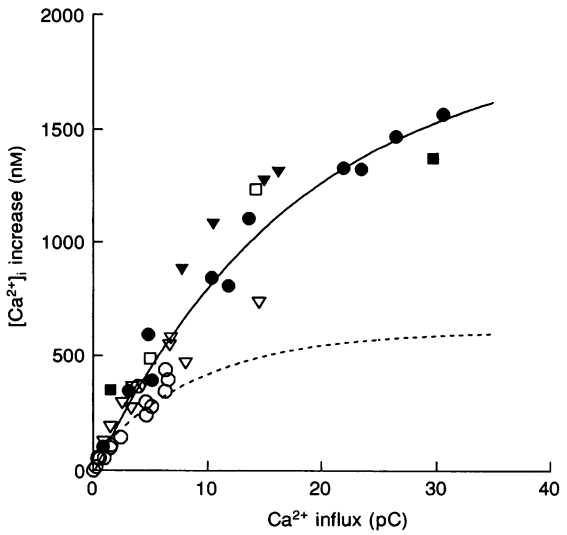

Figure 8. Effect of Ruthenium Red on the Ca^{2+} influx–$[Ca^{2+}]_i$ relationship
Ruthenium Red (10 μM) was included in the pipette solution. Data were obtained from 6 separate nerve endings, each indicated by a different symbol, exposed to various step depolarization-evoked Ca^{2+} loads. Continuous line represents a single exponential fit to all data points. Dashed line shows the exponential fit obtained from the data shown in Fig. 6*C* in the absence of Ruthenium Red.

illustrates the relationship between the increase in $[Ca^{2+}]_i$ and calcium influx for nerve endings dialysed with Ruthenium Red. In the presence of the mitochondrial Ca^{2+} uptake inhibitor the increase in $[Ca^{2+}]_i$ was found to be closely proportional to time integrated calcium currents of up to 30 pC and resulted in increases in averaged $[Ca^{2+}]_i$ of up to 1·5 μM. These results suggest mitochondria may provide an important role in buffering $[Ca^{2+}]_i$ in secretory nerve endings in response to large Ca^{2+} loads.

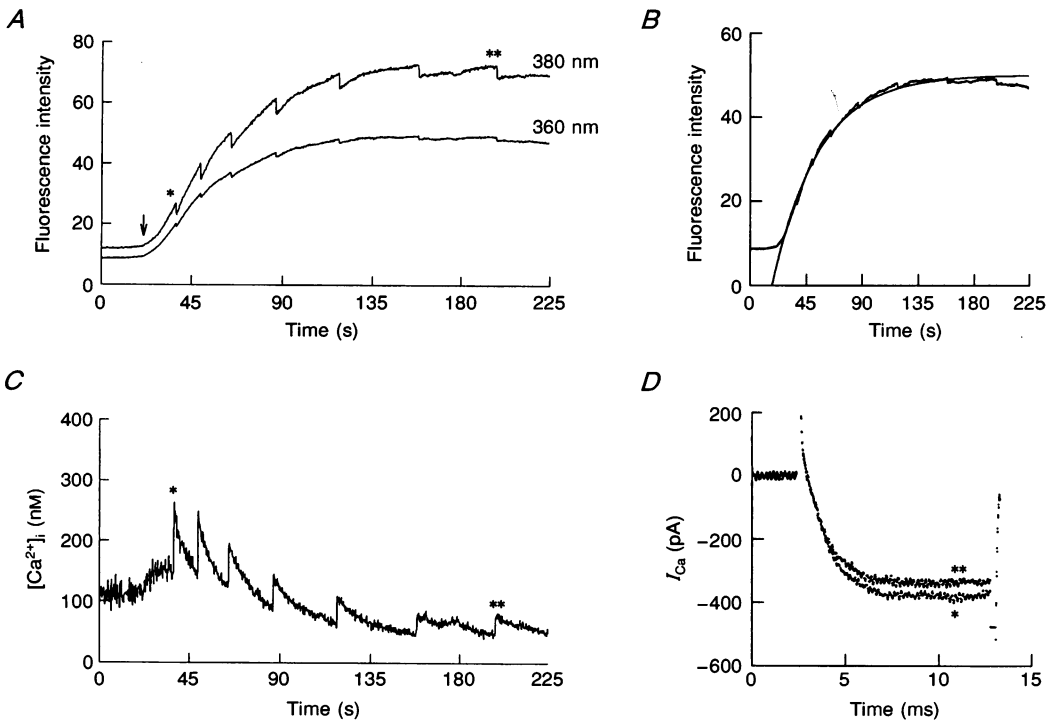

Figure 9. Effects of loading a nerve ending with buffering concentrations of fura-2 on depolarization-evoked Ca^{2+} transients
A, record of fura-2 (800 μM) fluorescence prior and immediately following attainment of a whole-cell recording configuration (arrow) at a Ca^{2+}-sensitive (380 nm) and Ca^{2+}-insensitive (365 nm) wavelength. *B*, exponential fit to change in fluorescence intensity at 365 nm following transition to whole-cell recording configuration. *C*, effect of seven brief (10 ms) depolarizing pulses to +10 mV (V_h = −90 mV) on $[Ca^{2+}]_i$ during fura-2 loading of the nerve ending. *D*, comparison of the evoked I_{Ca} to the first (* throughout) and last step (** throughout) depolarization during fura-2 loading of the nerve ending.

Determination of endogenous buffer capacity of nerve endings

In spite of the close relationship between the amplitude of the calcium current and the change in $[Ca^{2+}]_i$ for time-integrated calcium currents less than 10 pC, the peak value of $[Ca^{2+}]_i$ attained was far less than predicted based on the total ion flux and the estimated volume of the nerve endings. Thus, for example, in a nerve terminal lacking Ca^{2+} buffers an influx of Ca^{2+} equivalent to 5 pC of charge into an 8 μm diameter nerve terminal should result in a change in $[Ca^{2+}]_i$ of approximately 97 μM according to the relationship: $[Ca^{2+}]_i = Q/2FV$, where Q represents charge in coulombs, F is Faraday's constant and V is the cytoplasmic volume. This is a value of $[Ca^{2+}]_i$ far greater than that observed experimentally. The discrepancy is further enhanced considering that approximately 25% of the volume of these isolated secretory nerve endings is occupied by secretory granules (Nordmann, 1977). The difference may be attributed to a very rapid component of cytoplasmic buffering that differs both mechanistically and kinetically from slower buffering mechanisms which act to sequester calcium into intracellular organelles or to mediate Ca^{2+} efflux from the cell. In order to determine the properties of this fast, endogenous cytoplasmic buffer in the isolated nerve endings and to assess its effect on the recorded changes in $[Ca^{2+}]_i$ we have used methodology recently developed by Neher & Augustine (1992). The methodological approach is based on competition for Ca^{2+} between the endogenous buffer and fura-2 introduced into the cell as an exogenous Ca^{2+} buffer via a patch pipette.

Figure 9 shows the effects of loading 800 μM fura-2 into a nerve terminal on step depolarization-induced changes in $[Ca^{2+}]_i$. Measurement of emitted light intensity at 360 nm monitors the time course of fura-2 dialysis from the pipette into the terminal cytoplasm, reaching a plateau when the pipette and cytoplasmic fura-2 concentrations are equal. The rate of fura-2 loading of the nerve ending on transition from a cell-attached to whole-cell recording configuration could be fitted with a single exponential allowing estimation of the fura-2 concentration at the time of the applied step depolarizations (Fig. 9*B*). The τ

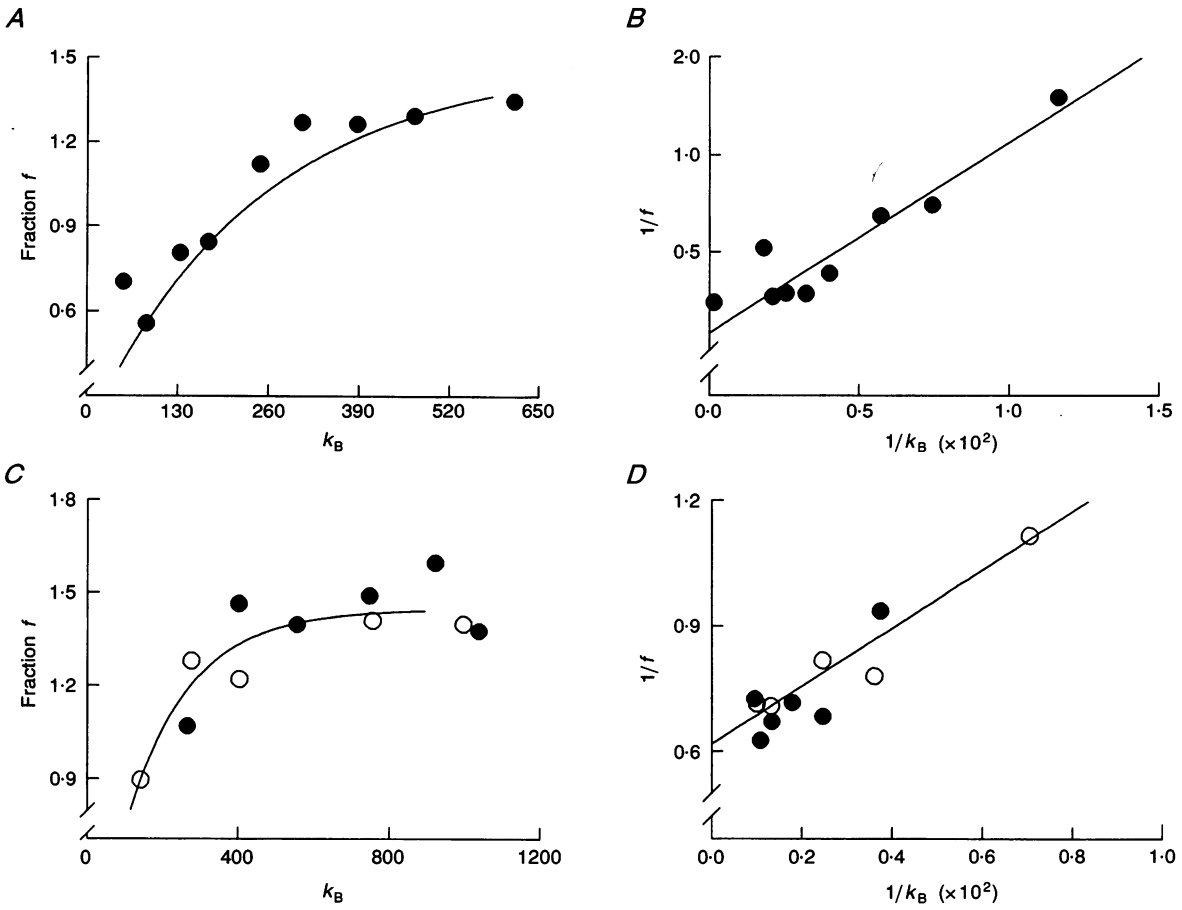

Figure 10. Representative relationships of the f value *versus* the Ca^{2+} binding capacity of fura-2 (k_B)

A, relationship of f *versus* k_B for a nerve ending loaded with 800 μM fura-2. *B*, double-reciprocal plot of data shown in *A*. Intercept with ordinate represents the value f_{max}. *C*, data pooled from two nerve endings (different symbols) loaded with 400 μM fura-2. *D*, double-reciprocal plot of data shown in *C*.

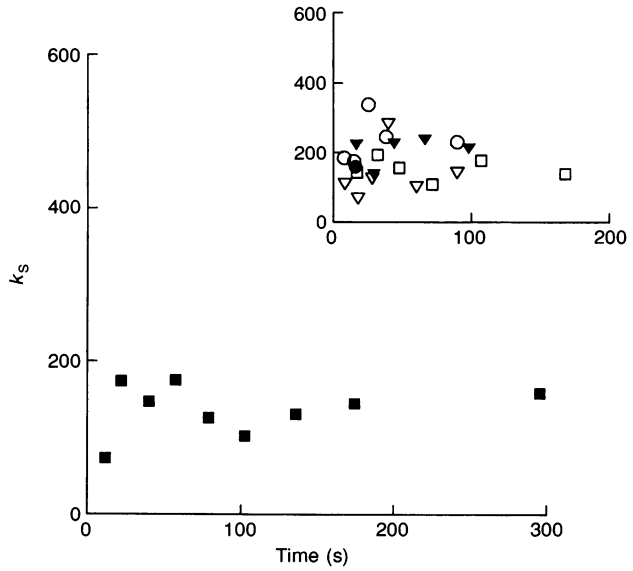

Figure 11. Stability of the endogenous Ca^{2+} binding capacity (k_S) during dialysis of the nerve ending with the patch pipette solution
The k_S value is plotted *versus* time since transition to whole cell recording configuration, for data from a single nerve ending. Inset shows similar data obtained from 4 other nerve endings.

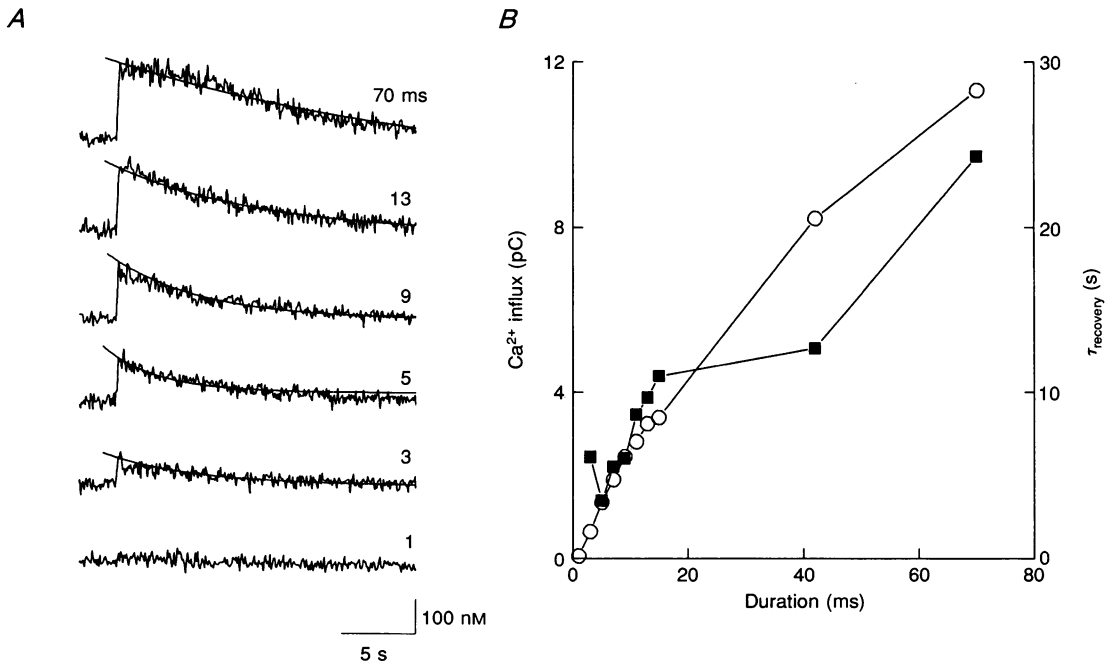

Figure 12. Relationship between the duration of an applied step depolarization and the time for recovery to resting $[Ca^{2+}]_i$ for a single nerve ending
A, $[Ca^{2+}]_i$ transients recorded in response to step depolarizations (−90 mV holding potential, +10 mV step potential) of equal amplitude but of increasing duration. Continuous, smooth lines show single exponential fit to the falling phase of the $[Ca^{2+}]_i$ transients. *B*, plot of Ca^{2+} influx and $[Ca^{2+}]_i$ recovery time constant *versus* the duration of the applied step depolarization. ■, $\tau_{recovery}$; ○, Ca^{2+} influx.

values for loading the nerve endings with fura-2 averaged 55 ± 7·4 s (mean ± S.E.M.; $n = 5$). As the fura-2 concentration within the nerve ending increased, the amplitude of the evoked change in $[Ca^{2+}]_i$ decreased and the time required for recovery to prestimulation $[Ca^{2+}]_i$ levels increased (Fig. 9*C*). The I_{Ca} evoked in response to the step depolarizations remained relatively constant over the duration of the recordings as evidenced by comparison of I_{Ca} from the first and last applied step depolarization (Fig. 9*D*). The time-dependent decrease in induced changes in $[Ca^{2+}]_i$ presumably resulted from the increasing competition between fura-2 and the endogenous buffer for entering calcium. The amount of calcium entering the nerve terminal during the step depolarizations which is bound to fura-2 is represented by the quantity f (see Methods and Neher & Augustine, 1992). The value of f is calculated from the change in emitted light intensity (ΔF_{380}, arbitrary units) over the integral of the I_{Ca} measured during the periods of applied step depolarizations. A plot of f *versus* the Ca^{2+} binding capacity of fura-2 (k_B) should presumably increase towards a plateau value. The intercept of the ordinate on a double-reciprocal plot provides the value f_{max}. Figure 10 shows representative data of the relationship of f and the Ca^{2+} binding capacity from nerve endings that were loaded with 400 or 800 μM fura-2. In both cases f reached plateau values (Fig. 10*A* and *C*) and the f_{max} values calculated from linear regression fits to the double-reciprocal plots were found to be 1·67 (Fig. 10*B*) and 1·7 (Fig. 10*D*). The values of f_{max} between nerve endings varied slightly ranging from 1·6 to 2·0 (1·76 ± 0·07, mean ± S.E.M.; $n = 5$). The values of k_S, the *endogenous* buffer capacity, were calculated from eqn (3). The average value of k_S, resulting from evaluation of several points across five separate nerve endings and combining data using 400 or 800 μM fura-2 was found to be 174·1 ± 17·6 (mean ± S.E.M.). Based on these values greater than 99% of the Ca^{2+} entering the nerve ending in response to step depolarizations is very rapidly buffered. These determinations were made at levels of Ca^{2+} influx where mitochondrial buffering is likely to be negligible. Figure 11 shows the relationship between k_S and the duration since transition to the whole cell recording configuration for each of the five terminals examined. The data suggest that over a period of at least 150 to 300 s the

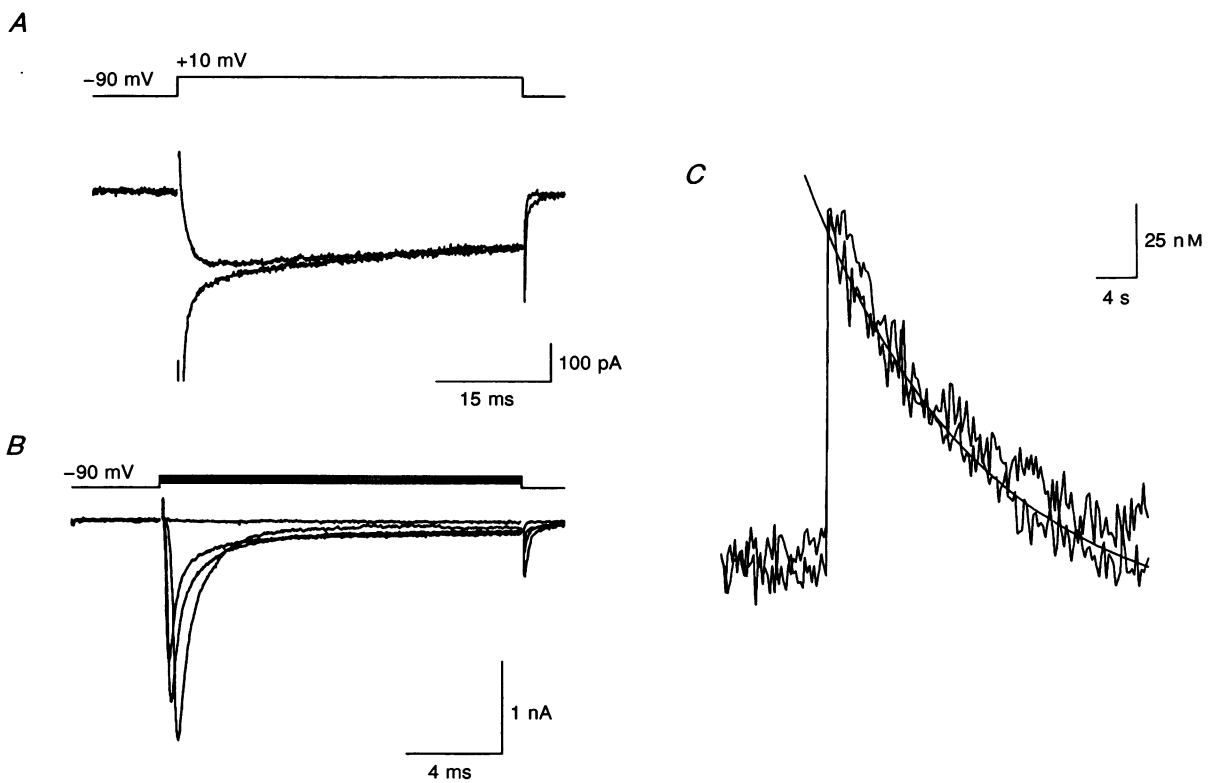

Figure 13. Effects of extracellular Na^+ on depolarization-induced increases in $[Ca^{2+}]_i$ and in recovery to basal $[Ca^{2+}]_i$

A, ionic currents evoked during step depolarizations to +10 mV from a holding potential of −90 mV in the absence and presence of 140 mM extracellular Na^+ ($[Ca^{2+}]_o = 10$ mM). *B*, reduced gain to show family of Na^+ currents in the presence of extracellular Na^+ evoked on step depolarizations from −50 to +10 mV in 20 mV increments from a holding potential of −90 mV. *C*, transient increases in $[Ca^{2+}]_i$ in the presence and absence of extracellular Na^+ evoked by the step depolarizations shown in *A*. Line on *C* represents single exponential fit of the control data.

k_S value for a given nerve ending remains relatively stable. This suggests that the fast endogenous cytoplasmic Ca^{2+} buffer is of low mobility either as a result of it being anchored within the nerve ending or of its being of large molecular mass.

Recovery of $[Ca^{2+}]_i$ following depolarization-evoked increase

The time required for return of $[Ca^{2+}]_i$ to baseline levels following a depolarization-evoked $[Ca^{2+}]_i$ increase far outlasted the duration of the applied step depolarization. Figure 12 shows that for brief step depolarizations there was a close correlation between the level of the evoked Ca^{2+} influx and the length of time required for recovery of basal $[Ca^{2+}]_i$. Variability existed between nerve endings with regard to the rate of recovery of resting $[Ca^{2+}]_i$ following an evoked increase. For a given nerve ending, the rate of recovery was found to be unaffected by return to holding potentials over the range of −90 to −50 mV following imposed step depolarizations. A number of Ca^{2+} sequestering and efflux mechanisms are present in nerve endings which may act in a homeostatic manner to bring about the return of $[Ca^{2+}]_i$ to a basal condition following an evoked $[Ca^{2+}]_i$ increase (Nordmann & Zyzek, 1982; Nicholls, 1989). However, the relative contribution of each mechanism to recovery of basal $[Ca^{2+}]_i$ following a depolarization-evoked increase is not well understood and may vary according to the type of nerve ending. A series of experiments were thus performed to investigate the relative contribution of a number of potential Ca^{2+} recovery mechanisms in these secretory nerve endings. In order to evaluate a possible contribution by Na^+–Ca^{2+} exchange, Ca^{2+} efflux was monitored in the presence or absence of extracellular sodium following depolarization evoked inward I_{Ca}. Extracellular Na^+ had no apparent effect on the peak amplitude or sustained component of the evoked I_{Ca} (Fig. 13*A*). However, in the presence of extracellular Na^+ large transient inward currents, attributable to activation of voltage-dependent Na^+ channels, were present (Fig. 13*B*). The recovery phase following the evoked $[Ca^{2+}]_i$ increases was unaffected by the extracellular Na^+, suggesting recovery to resting

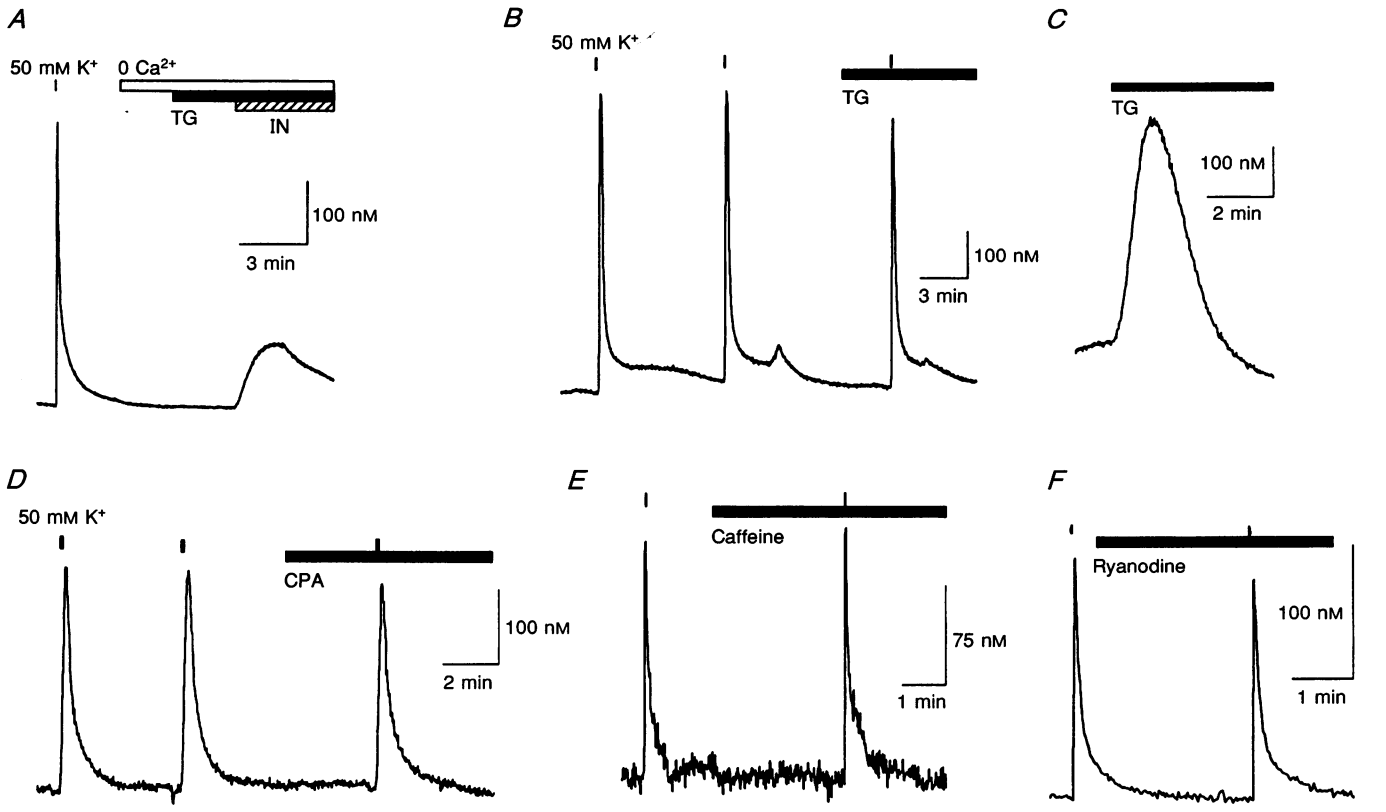

Figure 14. Effects of the intracellular Ca^{2+} pump inhibitors thapsigargin and cyclopiazonic acid on Ca^{2+} regulation in intact nerve endings

Effects of thapsigargin (TG, 2 μM; *A* and *B*) and cyclopiazonic acid (CPA, 30 μM; *D*) on basal $[Ca^{2+}]_i$, depolarization-induced changes in $[Ca^{2+}]_i$ and rates of recovery of resting $[Ca^{2+}]_i$ following an induced $[Ca^{2+}]_i$ increase. Ionomycin (IN, 5 μM) was added as indicated. *C*, thapsigargin (2 μM) mobilization of calcium from intracellular stores of rat pancreatic acinar cell measured in the absence of extracellular calcium (no added calcium plus 1 mM EGTA). Lack of effect of caffeine (10 mM; *E*) or ryanodine (1 μM; *F*) on Ca^{2+} regulation in an intact nerve endings. All solution changes are as indicated by bars above plots.

$[Ca^{2+}]_i$ was mediated, under these recording conditions, primarily by Na^+-independent mechanisms. These data also indicate that the TEA-containing bath solutions used in the present study did not adversely affect the Ca^{2+} recovery mechanisms or the resting $[Ca^{2+}]_i$.

Thapsigargin and cyclopiazonic acid are known to inhibit specifically ATP-dependent Ca^{2+} pumps localized on calcium-storing intracellular compartments such as the smooth endoplasmic reticulum and are without effect on the ATP-dependent Ca^{2+} pumps of the plasmalemma. The possible involvement of intracellularly localized ATP-dependent pumps, as homeostatic mechanisms operating to sequester Ca^{2+} following evoked $[Ca^{2+}]_i$ increases, was tested on preparations of intact, dissociated nerve endings. In these experiments the nerve endings were loaded with fura-2 using the acetoxymethyl ester derivative (fura-2 AM) and depolarized, under constant superfusion, by brief exposures to depolarizing concentrations (50 mM) of elevated K^+. Figure 14 shows that treatment of nerve endings with concentrations of thapsigargin (2 μM) or cyclopiazonic acid (30 μM) that exhibit maximal effects on other cell types had no effect on resting $[Ca^{2+}]_i$, depolarization evoked increases in $[Ca^{2+}]_i$, or on the rate of recovery of $[Ca^{2+}]_i$ to basal values in the nerve endings. Note that similar pharmacological treatment in pancreatic acinar cells was effective to mobilize Ca^{2+} from intracellular stores (Fig. 14*C*). Application of ionomycin following thapsigargin treatment of the nerve endings maintained in Ca^{2+}-free conditions resulted in a transient increase in $[Ca^{2+}]_i$. These data indicate that intracellular ATP-dependent Ca^{2+}

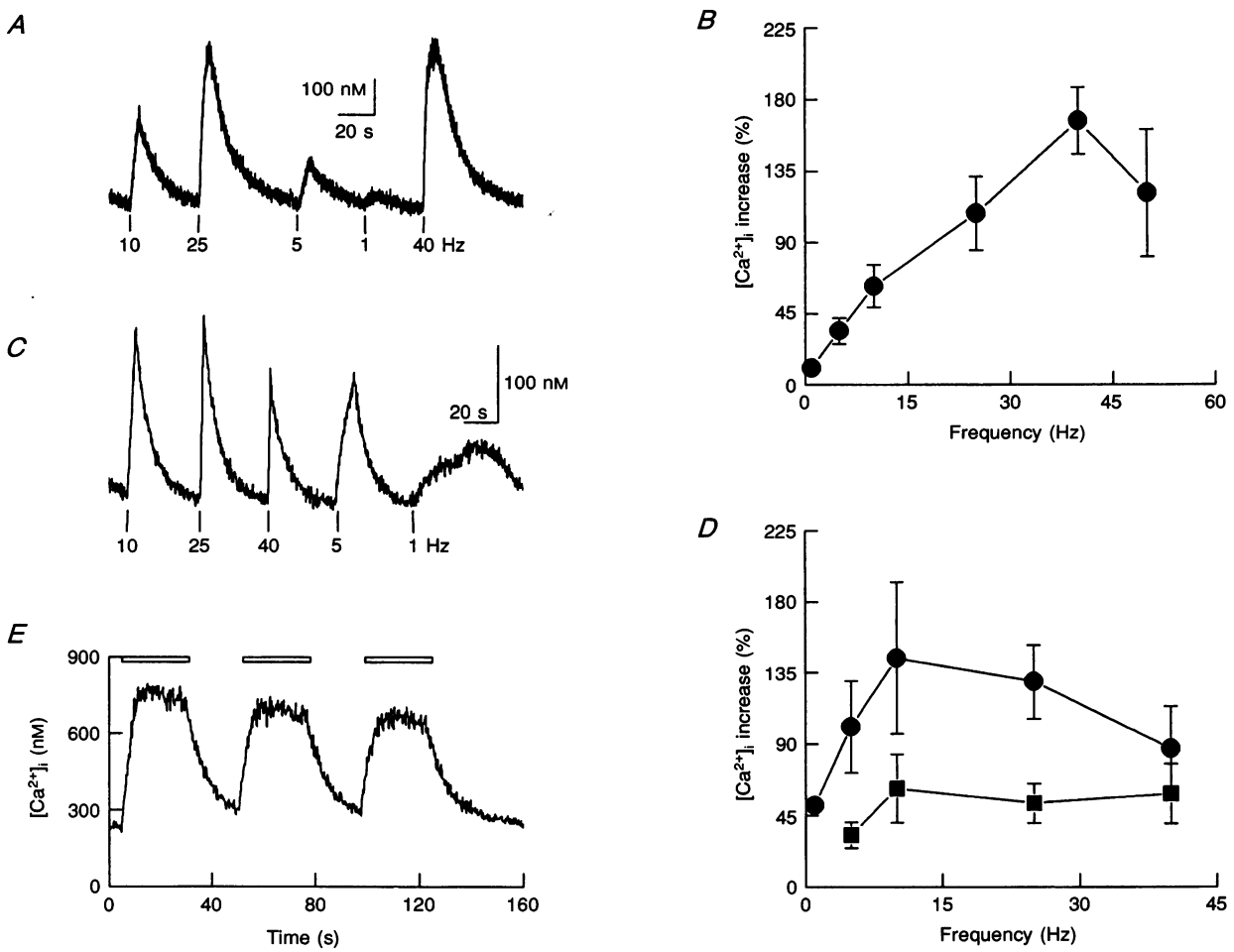

Figure 15. Effect of repetitive step depolarizations on $[Ca^{2+}]_i$

A, effect of a constant period of stimulation (5 s) at indicated pulse frequencies on $[Ca^{2+}]_i$ in a single nerve ending ($V_h = -90$ mV). *B*, averaged data obtained from 5 nerve endings for stimulation protocol given in *A*. *C*, effects of a constant number of stimuli (50 pulses) applied at indicated frequencies on $[Ca^{2+}]_i$ in a single nerve ending ($V_h = -90$ mV). *D*, averaged data for the stimulation protocol given in *C* (■, $V_h = -50$ hold, $n = 3$; ●, $V_h = -90$ hold, $n = 3$). *E*, effect of step depolarizations applied at mean frequencies (13 Hz) and durations (26 s) as occur *in vivo* in vasopressinergic neurons during impulse bursting on $[Ca^{2+}]_i$. Three stimulation periods (open bars) were applied with an interburst interval of 21 s. In all experiments in this figure, step depolarizations were to +10 mV and pipette [fura-2] was 150 μM. Each pulse was 2 ms in duration.

pumps are either not a major pathway of $[Ca^{2+}]_i$ regulation in these secretory nerve terminals or that the intracellular Ca^{2+} pumps in these nerve endings are of different pharmacological sensitivity than those characterized from a wide variety of cell types.

An additional series of experiments investigated the possibility that these secretory nerve endings possess a caffeine- or ryanodine-sensitive intracellular calcium store. These compounds have been routinely used to indicate the presence of a calcium-induced calcium release (CICR) mechanism and will act to discharge this intracellular calcium pool. The presence of a such a pool could act to augment the $[Ca^{2+}]_i$ signal during Ca^{2+} influx as well as to participate in Ca^{2+} sequestration. Treatment of the nerve endings with caffeine or ryanodine either alone (Fig. 14*D* and *E*) or in combination had no apparent effects on basal $[Ca^{2+}]_i$ or on depolarization-induced $[Ca^{2+}]_i$ increases.

Ca^{2+} transients induced by repetitive step depolarizations

The effects of repetitive step depolarizations under voltage clamp on $[Ca^{2+}]_i$ were investigated to determine the frequency dependence of changes in $[Ca^{2+}]_i$ and to begin to evaluate whether mitochondrial buffering of $[Ca^{2+}]_i$ may play a homeostatic role during physiological impulse bursting. Brief depolarizing steps (−90 to +10 mV, 2 ms duration) given over a period of 5 s increased $[Ca^{2+}]_i$ in proportion to the applied frequency up to 25 Hz (Fig. 15*A* and *B*). Moreover, the rate of rise in $[Ca^{2+}]_i$ increased as the stimulation frequency increased. However, when a constant number of pulses were given over the same frequency range, 40 Hz stimulation gave consistently lower increases in $[Ca^{2+}]_i$ than did 10 Hz stimulation on steps from −90 but not from −50 mV holding potentials (Fig. 15*C* and *D*). Note that stimulation at frequencies as low as 1 Hz resulted in a noticeable increase in the $[Ca^{2+}]_i$.

In response to physiological demand for vasopressin and oxytocin the magnocellular neurones in the hypothalamus exhibit a change in their impulse firing pattern from a slow tonic firing to a phasic discharge pattern (Poulain & Wakerley, 1982). The oxytocin and vasopressin neurones show characteristically different phasic impulse patterns. An oxytocin-containing cell can undergo a bursting discharge of impulses reaching frequencies as high as 80 Hz for 0·5 to 4 s, whereas vasopressin-containing cells characteristically show a lower mean phasic impulse firing frequency of approximately 13 Hz over a period averaging 26 s. The effect of step depolarizations mimicking the average impulse discharge frequency and duration of an AVP neurone on $[Ca^{2+}]_i$ is shown in Fig. 15*E*. Onset of the step depolarizations led to a rapid rise in $[Ca^{2+}]_i$ which quickly reached a plateau value at which it was maintained until the pulses ceased. Note that an intraburst period of 21 s allowed for nearly complete recovery of $[Ca^{2+}]_i$ to basal values under these recording conditions. The rise and recovery in $[Ca^{2+}]_i$ could be repetitively reproduced by subsequent stimulation periods. The plateau $[Ca^{2+}]_i$ level reached was, however, dependent upon the strength of the applied depolarization as step depolarizations to +10 mV resulted in plateau values greater than steps to −10 mV even within the same nerve ending.

DISCUSSION

In this paper we have examined the properties of cytosolic Ca^{2+} buffering and Ca^{2+} regulation in single dissociated nerve endings from vasopressin- and oxytocin-containing hypothalamic magnocellular neurones. The studies used simultaneous measurements of Ca^{2+} influx (I_{Ca}) under voltage clamp via the whole-cell recording configuration of the patch clamp technique and of changes in $[Ca^{2+}]_i$ using microspectrofluorimetry of fura-2. Application of brief step depolarizations revealed three distinct rapid cytosolic Ca^{2+} buffering processes. One of these represented rapid binding of Ca^{2+} to immobile or slowly diffusible endogenous buffers. This buffer component was probably represented by the reversible interaction of Ca^{2+} with a class of high-affinity Ca^{2+} binding proteins. A second rapid Ca^{2+} buffering process became apparent when the Ca^{2+} load applied to a nerve ending raised $[Ca^{2+}]_i$ within a given concentration range. This buffering mechanism was of lower affinity but of high capacity and was found to be sensitive to the mitochondrial Ca^{2+} uptake inhibitor Ruthenium Red. A third buffering mechanism was represented by energy-dependent Ca^{2+} efflux from the nerve ending. Repetitive step depolarizations, mimicking in frequency and duration the phasic discharge of impulses occurring in AVP neurones (Poulain & Wakerley, 1982) was found to increase the $[Ca^{2+}]_i$ to values where buffering by each of these mechanism occurs.

Multiple sites of Ca^{2+} buffering have been previously reported based largely on radiotracer flux measurements of studies of intact and disrupted axonal or synaptosome preparations. The buffering mechanisms identified include cytosolic proteins that exhibit specific binding for Ca^{2+} (Van Eldik, Zendegui, Marshak & Watterson, 1982) and binding to Ca^{2+} transport proteins such as Na^+–Ca^{2+} exchange (Blaustein & Ector, 1976) and ATP-dependent Ca^{2+} pumps (Blaustein, Ratzlaff, Kendrick & Schweitzer, 1978*a*). In addition, cytosolic Ca^{2+} loads in nerve endings have been reported to be buffered by Ca^{2+} sequestration into both mitochondrial and non-mitochondrial intracellular compartments (Blaustein *et al.* 1978*a*, *b*). The relative contribution of these various buffering components in determining the amplitude, shape and duration of an induced Ca^{2+} load, as occurs physiologically during action potential invasion of the nerve terminal, remains unclear. Moreover, the mechanisms involved may vary with the specific nerve ending type. For example, substantial variation exists among studies with regard to the importance ascribed to Na^+–Ca^{2+} exchange activity in

recovery from Ca^{2+} loads and in regulating the resting $[Ca^{2+}]_i$ (Nachshen, 1985; Nicholls 1989). In addition, while ATP-dependent Ca^{2+} sequestration into intracellular compartments has been suggested from studies on disrupted synaptosome preparations (Blaustein, Ratzlaff & Schweitzer, 1978*b*) the generality and the subcellular site of this mechanism remains unclear. The results of the present study, and of our previous work (Stuenkel, 1990), suggest that Na^+–Ca^{2+} exchange in neurohypophysial nerve endings may play little, if any, role in regulating $[Ca^{2+}]_i$. The experimental results also argue against a significant ATP-dependent intracellular Ca^{2+} sequestering mechanism based, in part, on data from pharmacological inhibitors of this class of ATP-dependent pumps. Our results are, however, consistent with multiple Ca^{2+} buffering mechanisms whose contribution is dependent upon the Ca^{2+} load and with Ca^{2+} recovery and homeostasis mediated largely by energy-dependent Ca^{2+} extrusion across the plasmalemma.

The diverse array of biological effects mediated by alterations in $[Ca^{2+}]_i$ occurs via transduction through reversible interactions with Ca^{2+} binding proteins, which thereby act as endogenous Ca^{2+} buffers. Competition for Ca^{2+} binding between these endogenous Ca^{2+} buffers and the exogenously introduced Ca^{2+} binding fluorescent indicator fura-2 can provide an estimate of k_S, the endogenous cytoplasmic Ca^{2+} binding capacity (Neher & Augustine, 1992; Zhou & Neher, 1993). The value calculated for k_S using this methodological approach in the isolated nerve endings was 174 and indicates that greater than 99% of depolarization-induced Ca^{2+} influx through the voltage-sensitive channels is rapidly bound to a high-affinity endogenous buffering component. This is consistent with previous findings of rapid and efficient Ca^{2+} buffering in the neuroendocrine chromaffin cells reported by Neher & Augustine (1992) as well as for Ca^{2+} buffering in sympathetic neurones (Thayer & Miller, 1990) and in isolated squid axons (Brinley, Tiffert, Scarpa & Mullins, 1977). Thus, in response to low levels of depolarization-induced Ca^{2+} influx, while a proportional increase in the intracellular calcium concentration was found, this was much less than predicted based on the charge redistribution and the estimated volume of the nerve ending. While there are a number of Ca^{2+} binding protein candidates which may act as efficient Ca^{2+} buffers, the specific Ca^{2+} binding proteins that dominate this buffer component remain unknown (Van Eldik *et al.* 1982). In spite of a lack of specific information many of the properties of this buffer component are likely to be similar to those of the prototypical Ca^{2+} binding protein calmodulin. For example, calmodulin is found in high concentrations in brain tissue (30 μM) and binds calcium (4 mole Ca^{2+} (mol protein)$^{-1}$) with dissociation constants in the micromolar range. Although a specific molecular identification of this buffer component cannot yet be made some general information can be derived from our results. The maintenance of the endogenous buffering capacity (k_S) at relatively stable values during continued dialysis from the patch pipette suggests the Ca^{2+} binding molecules responsible are either membrane anchored, rendering them immobile, or are of large molecular mass. A limiting mass of 125 kDa was estimated based on the relationship developed by Pusch & Neher (1988) for rates of diffusional exchange between a cell and a patch pipette and assuming a series conductance of 100 nS. The diffusional characteristics of this endogenous Ca^{2+} buffer are similar to those previously detailed for chromaffin cells (Neher & Augustine, 1992).

In the presence of larger Ca^{2+} loads the relationship between the time-integrated I_{Ca} and the increase in $[Ca^{2+}]_i$ approached an asymptote, the two thereby ceasing to be proportional. Once stimulation has raised $[Ca^{2+}]_i$ by about 600 nM, augmenting I_{Ca} by as much as 4-fold makes little further change in the spatially averaged $[Ca^{2+}]_i$. These data indicate that an additional buffering component, which greatly increases the apparent cytoplasmic Ca^{2+} buffering capacity, becomes active once a $[Ca^{2+}]_i$ set-point is reached. The $[Ca^{2+}]_i$ value of this set-point is at approximately 0·85–1 μM free calcium, taking into consideration a resting value of calcium, in 10 mM extracellular Ca^{2+}, of 250 nM. Evidence that this buffering component represents a distinct mechanism from that of the endogenous cytoplasmic buffering capacity described above is based on the abrupt loss of I_{Ca} *versus* $[Ca^{2+}]_i$ proportionality at a set point and by the loss of the second buffering component in the presence of Ruthenium Red. While the mechanism responsible for this Ca^{2+} buffering component has not been identified its properties are consistent with mitochondrial Ca^{2+} uptake, although Ruthenium Red has been reported to alter Ca^{2+} uptake by secretory granules and to blockade ryanodine receptors. Mitochondria are commonly distributed among an abundance of neurosecretory granules that dominate electron micrograph profiles of the cytoplasm of the isolated neurosecretosomes (Nordmann, 1977).

Calcium accumulation by mitochondria results from the generation of an electrochemical gradient via operation of the electron transport chain. The relevance of this mechanism at $[Ca^{2+}]_i$ that occur over the physiological range has been repeatedly discussed (Brinley *et al.* 1977; Blaustein, Ratzlaff & Schweitzer, 1978*b*; Nicholls, 1989). For example, in the absence of stimulus-evoked Ca^{2+} influx, i.e. the resting state, intramitochondrial calcium in various cell types and in synaptosome preparations is low, suggesting that mitochondria do not form a major component in regulation of resting $[Ca^{2+}]_i$. Thus, in the resting state, treatments which presumably would release mitochondrially stored calcium, such as elevation of intracellular $[Na^+]_i$, application of Ca^{2+} ionophores, poisoning of the electron transport chain or direct pharmacological dissipation of the mitochondrial electrochemical gradient, do not raise $[Ca^{2+}]_i$ in a manner consistent with release of stored Ca^{2+} from the mitochondria (Nicholls, 1989). Our

previous work (Stuenkel & Nordmann, 1993*b*), together with data presented here (see below), also indicates that under resting conditions there exists only small quantities of releasable Ca^{2+} in intracellular Ca^{2+} stores in the neurohypophysial nerve endings. In addition, the relationship between Ca^{2+} influx and increase in $[Ca^{2+}]_i$ was unchanged for small Ca^{2+} loads in the presence of Ruthenium Red, thereby supporting a lack of significant Ca^{2+} buffering by mitochondria at low Ca^{2+} loads. This occurs in spite of a significant leak of $[Ca^{2+}]_i$ into the nerve terminals at rest as indicated by the observed sensitivity of $[Ca^{2+}]_i$ to $[Ca^{2+}]_o$. The continual cycling of calcium across the plasma membrane under resting conditions allows for the precise regulation of $[Ca^{2+}]_i$ at a point where efflux mechanisms exactly offset influx, thereby maintaining a constant Ca^{2+} electrochemical gradient (Nicholls, 1989).

The Ruthenium Red-sensitive (i.e. presumed mitochondrial) Ca^{2+} uptake mechanism may also participate, along with Ca^{2+} efflux via the plasma membrane Ca^{2+} pump, in limiting the rise in intraterminal $[Ca^{2+}]$ in response to application of repetitive step depolarizations. While the increase in $[Ca^{2+}]_i$ under these conditions was found to be dependent upon the applied frequency, the increase in $[Ca^{2+}]_i$ per impulse was found to decrease at higher frequencies. These results are consistent with the frequency dependence of vasopressin secretion from isolated neural lobes (Cazalis, Dayanithi & Nordmann, 1985; Nordmann & Stuenkel, 1986). Interestingly, application of step depolarizations that mimic, in mean frequency and duration, the impulse firing during AVP-like bursts raised $[Ca^{2+}]_i$ to levels where mitochondrial buffering may occur. Furthermore, the increase in $[Ca^{2+}]_i$ observed here is likely to underestimate the averaged cytosolic $[Ca^{2+}]_i$ increase in intact nerve endings during action potential invasion as a result of broadening of action potentials in these nerve endings during repetitive firing (Bourque, 1990) and the lack of buffering by diffusion of Ca^{2+} into the patch pipette over a 25–30 s stimulation period. These data suggest that intraterminal mitochondria serve an important physiological role in limiting the rise in $[Ca^{2+}]_i$. This mechanism avoids conditions of pathological Ca^{2+} overload while allowing $[Ca^{2+}]_i$ to rise sufficiently to initiate exocytosis. It should be noted, however, that the establishment of a plateau $[Ca^{2+}]_i$ to repetitive stimulation occurring over periods of seconds was not entirely dependent upon mitochondrial Ca^{2+} buffering as $[Ca^{2+}]_i$ plateaux were observed under conditions where the repetitive stimulus-evoked $[Ca^{2+}]_i$ increases did not reach the mitochondrial Ca^{2+} uptake set-point. The generation of the plateau $[Ca^{2+}]_i$ in response to repetitive stimuli applied over seconds is likely to result from a situation where Ca^{2+} influx is equal to the combined effects of efflux and sequestration. The Ca^{2+} efflux, in this situation, is probably represented by the activity of the plasma membrane Ca^{2+} pump. The low levels of intracellularly sequestered free Ca^{2+} in nerve endings prior to stimulation (Fig. 14*A* and Stuenkel & Nordmann, 1993*b*) suggests that calcium sequestered intracellularly during stimulation is given up from these stores following stimulation and effluxed from the nerve ending.

Ca^{2+} mobilization from intracellular stores

Mobilization of calcium from intracellular stores can occur through activation of calcium channels gated by IP_3, cADP-ribose or calcium, the latter being sensitive to ryanodine and caffeine. Multiple isoforms of both IP_3 and ryanodine receptors have been reported in neural tissue and a number of reports have demonstrated their involvement in receptor- or depolarization-mediated Ca^{2+} signals in neural cells (Kuba & Nishi, 1976, Friel & Tsien, 1992). In addition, secretory granules often have a high intragranular Ca^{2+} content, a fraction of which may exist as free calcium ions and which may, potentially, be altered by secretory stimuli (Nicaise, Maggio, Thirion, Horoyan & Keicher, 1992). The close correspondence between depolarization-evoked inward Ca^{2+} currents and changes in $[Ca^{2+}]_i$ in our findings in the neurohypophysial nerve endings argues against a contribution of these Ca^{2+} mobilizing mechanisms to recorded Ca^{2+} signals. Membrane depolarization in the absence of Ca^{2+} influx was also found to be ineffective at mobilizing Ca^{2+} from intracellular Ca^{2+} stores. The above findings are consistent with evidence showing a close correlation of the evoked Ca^{2+} currents to neurotransmitter release and the necessity for Ca^{2+} influx, and not membrane depolarization alone, to induce exocytotic neurotransmitter release (Augustine *et al.* 1987).

A small rise in intracellular calcium could be detected upon treatment of the nerve endings with the Ca^{2+} ionophore ionomycin, in the absence of extracellular Ca^{2+}, demonstrating our ability to resolve the release of intracellular stored calcium in the nerve endings. The relatively small amplitude of the Ca^{2+} signal from ionomycin-releasable calcium stores compared with depolarization-evoked increases in $[Ca^{2+}]_i$, however, indicates that these nerve endings, in the resting state, do not have extensive releasable intracellular Ca^{2+} stores. As Ca^{2+} uptake and sequestration into intracellular Ca^{2+} stores is largely mediated by energy-dependent calcium pumps, often termed smooth endoplasmic reticulum calcium pumps or SERCA Ca^{2+}-ATPases, inhibition of these pumps would be expected to generate a rise in $[Ca^{2+}]_i$ via leak of sequestered Ca^{2+} from the store. The lack of effects on basal or stimulated $[Ca^{2+}]_i$ on treatment with the selective SERCA pump inhibitors thapsigargin or cyclopiazonic acid on intact nerve endings is consistent with an absence of IP_3- or ryanodine-sensitive Ca^{2+} stores in the nerve endings. Similar treatments on pancreatic acini, which possess IP_3-sensitive Ca^{2+} stores, led to the expected rise in $[Ca^{2+}]_i$. These data also suggest that Ca^{2+} sequestration by SERCA activity plays little, if any, role in recovery of resting $[Ca^{2+}]_i$ following a depolarization-induced Ca^{2+} load. As a number of specific isoforms of the SERCA pumps have been reported, an alternative

explanation is that an isoform exists in nerve endings that is pharmacologically unique. It should also be noted that although multiple Ca^{2+} efflux mechanisms have been demonstrated in neurohypophysial nerve endings (Nordmann & Zyzek, 1982) the rapid recovery to basal $[Ca^{2+}]_i$ levels following an induced $[Ca^{2+}]_i$ increase was largely unaffected by the extracellular Na^+ concentration. These data argue against a major role for the electrogenic Na^+–Ca^{2+} exchanger in Ca^{2+} recovery or in maintaining low basal $[Ca^{2+}]_i$ levels and indicate, in this regard, a predominant role for the plasma membrane Ca^{2+}-ATPase.

Relevance of Ca^{2+} buffering mechanisms to neurohormone secretion

In conclusion, the results of this paper demonstrate the existence of three distinct endogenous Ca^{2+} buffer components in neurohypophysial nerve endings. These data may explain the importance of phasic impulse bursting to potentiation of release of the neuropeptides oxytocin and vasopressin from this system. An induction of cell-specific impulse bursting patterns is characteristic of the magnocellular neurosecretory cells in response to physiological demand for release of vasopressin or oxytocin (Poulain & Wakerley, 1982). The rhythmic bursting leads to potentiation of vasopressin secretion over a pattern of continuous stimulation containing the same number of stimuli. A number of characteristics of the recurring periods of phasic impulse firing are important for the potentiating effects on release, including impulse frequency within the burst, burst duration and the silent period between bursts (Cazalis, Dayanithi & Nordmann, 1985). The strict relationship between a rise in $[Ca^{2+}]_i$ and initiation of secretion suggests that the phasic firing pattern enhances the resulting intracellular Ca^{2+} signal. Measurements of $[Ca^{2+}]_i$ in these nerve endings have previously shown a frequency-dependent increase in $[Ca^{2+}]_i$ that closely correlates to the frequency dependence of the AVP secretory response (Brethes, Dayanithi, Letellier & Nordmann, 1987; Jackson, Konnerth & Augustine, 1991). A maintained increase in the $[Ca^{2+}]_i$ alone is not, however, capable of sustaining vasopressin release. For continued secretion of vasopressin, periodic changes in intracellular calcium are required (Stuenkel & Nordmann, 1993*a*). In addition, analysis of the secretory characteristics from single neurohypophysial nerve endings, by monitoring of membrane capacitance simultaneously with measurements of intracellular calcium, suggest that spatially averaged $[Ca^{2+}]_i$ levels within the range of 500–700 nM accompany the induction of exocytosis (Lindau, Stuenkel & Nordmann, 1992). The results presented here show that application of repetitive step depolarizations that mimic in frequency and duration that of an AVP burst of action potentials rapidly raised the averaged $[Ca^{2+}]_i$ to these levels and then plateaued. It is likely that $[Ca^{2+}]_i$ reached a plateau as a result of $[Ca^{2+}]_i$ reaching the set point for induction of the Ruthenium Red-sensitive (e.g. mitochondrial) uptake mechanism, which provides a temporary high-capacity Ca^{2+} sink, and by Ca^{2+}-dependent stimulation of the plasma membrane Ca^{2+} pump. The characteristics of these buffers, therefore, allow $[Ca^{2+}]_i$ to rise sufficiently to initiate secretion but act in a protective manner to avoid a pathological Ca^{2+} overload in the nerve ending. Interestingly, the $[Ca^{2+}]_i$ was observed to plateau prior to the cessation of stimuli within a burst. Moreover, the increase in $[Ca^{2+}]_i$ observed in response to repetitive step depolarizations under voltage clamp is likely to underestimate the Ca^{2+} load generated by action potentials in these nerve endings at similar frequencies resulting, in part, from spike broadening. Thus, continued impulse activity would result in a stable, maintained elevated $[Ca^{2+}]_i$, a condition disadvantageous for continued neurohormone secretion. Indeed, measurements of exocytotic activity at the level of single neurohypophysial nerve endings have shown that repetitive firing leads initially to facilitation of the exocytotic response followed shortly thereafter by a decrease in the secretory response (Fidler Lim, Nowycky & Bookman, 1990). The decrease in secretion does not apparently result from depletion of immediately releasable neurosecretory granules (Stuenkel & Nordmann, 1993*a*). The interburst period, therefore, allows for a period during which Ca^{2+} can recover towards resting levels prior to invasion of the next phasic discharge of impulses. Intracellularly sequestered Ca^{2+} may also be given up and effluxed during this period or over a slower time course following completion of repetitive bursting activity. In this manner the $[Ca^{2+}]_i$ is repetitively raised to near maximal averaged $[Ca^{2+}]_i$ values at a periodicity nearly optimal to sustain secretion (Nordmann & Stuenkel, 1986; Stuenkel & Nordmann, 1993*a*). The results presented here would suggest that recovery of $[Ca^{2+}]_i$ occurs predominantly via a plasma membrane ATP-dependent Ca^{2+} pump and not via uptake into intracellular Ca^{2+} stores or by efflux through a plasma membrane Na^+–Ca^{2+} exchange transport process.

REFERENCES

Ahmed, Z. & Conner, J. A. (1988). Calcium regulation by and buffer capacity of molluscan neurones during calcium transients. *Cell Calcium* **9**, 57–69.

Artalejo, C. R., Adams, M. E. & Fox, A. P. (1994). Three types of Ca^{2+} channel trigger secretion with different efficacies in chromaffin cells. *Nature* **367**, 72–76.

Augustine, G. J., Charlton, M. P. & Smith, S. J. (1987). Calcium action in synaptic transmitter release. *Annual Review of Neuroscience* **10**, 633–693.

Augustine, G. J. & Neher, E. (1992). Calcium requirements for secretion in bovine chromaffin cells. *Journal of Physiology* **450**, 247–271.

Baker, P. F. & McNaughton, P. A. (1976). Kinetics and energetics of calcium efflux from intact squid giant axons. *Journal of Physiology* **259**, 103–144.

Blaustein, M. P. & Ector, A. C. (1976). Carrier-mediated sodium-dependent and calcium-dependent calcium efflux from pinched-off presynaptic nerve terminals (syaptosomes) *in vitro*. *Biochimica et Biophysica Acta* **419**, 295–308.

Blaustein, M. P., Ratzlaff, R. W., Kendrick, N. C. & Schweitzer, E. S. (1978*a*). Calcium buffering in presynaptic nerve terminals. I. Evidence for involvement of a nonmitochondrial ATP-dependent sequestration mechanism. *Journal of General Physiology* **72**, 15–41.

Blaustein, M. P., Ratzlaff, R. W. & Schweitzer, E. S. (1978*b*). Calcium buffering in presynaptic nerve terminals. II. Kinetic properties of the nonmitochondrial Ca sequestration mechanism. *Journal of General Physiology* **72**, 43–66.

Bourque, C. W. (1990). Intraterminal recordings from the rat neurohypophysis *in vitro*. *Journal of Physiology* **421**, 247–262.

Brethes, D., Dayanithi, G., Letellier, L. & Nordmann, J. J. (1987). Depolarization-induced Ca^{2+} increase in isolated neurosecretory nerve terminals measured with fura-2. *Proceedings of the National Academy of Sciences of the USA* **84**, 1439–1443.

Brinley, F. J. Jr, Tiffert, T., Scarpa, A. & Mullins, L. J. (1977). Intracellular calcium buffering capacity in isolated squid axons. *Journal of General Physiology* **70**, 355–384.

Cazalis, M., Dayanithi, G. & Nordmann, J. J. (1985). The role of patterned burst and interburst interval on the excitation-coupling mechanism in the isolated rat neural lobe. *Journal of Physiology* **369**, 45–60.

Cazalis, M., Dayanithi, G. & Nordmann, J. J. (1987). Hormone release from isolated nerve endings of the rat neurohypophysis. *Journal of Physiology* **390**, 55–70.

Dayanithi, G., Martin-Moutot, N., Barlier, S., Colin, D. A., Kretz-Zaepfel, M., Couraud, F. & Nordmann, J. J. (1988). The calcium channel antagonist conotoxin inhibits secretion from peptidergic nerve terminals. *Biochemical and Biophysical Research Communications* **156**, 255–262.

Fidler Lim, N., Nowycky, M. C. & Bookman, R. J. (1990). Direct measurement of exocytosis and calcium currents in single vertebrate nerve terminals. *Nature* **344**, 449–451.

Friel, D. D. & Tsien, R. W. (1992). A caffeine- and ryanodine-sensitive Ca^{2+} store in bullfrog sympathetic neurones modulates effects of Ca^{2+} entry of $[Ca^{2+}]_i$. *Journal of Physiology* **450**, 217–246.

Grynkiewicz, G., Poenie, M. & Tsien, R. Y. (1985). A new generation of Ca indicators with greatly improved fluorescent properties. *Journal of Biological Chemistry* **260**, 3440–3450.

Hamill, O. P., Marty, A., Neher, E., Sakmann, B. & Sigworth, F. J. (1981). Improved patch-clamp techniques for high-resolution current recording from cells and cell-free membrane patches. *Pflügers Archiv* **391**, 85–100.

Jackson, M. B., Konnerth, A. & Augustine, G. J. (1991). Action potentials broadening and frequency-dependent facilitation of calcium signals in pituitary nerve terminals. *Proceedings of the National Academy of Sciences of the USA* **88**, 381–384.

Katz, B. & Miledi, R. (1967). The timing of calcium action during neuromuscular transmission. *Journal of Physiology* **189**, 535–544.

Kuba, K. & Nishi, S. (1976). Rhythmic hyperpolarizations and depolarization of sympathetic ganglion cells induced by caffeine. *Journal of Neurophysiology* **39**, 547–563.

Lemos, J. R. & Nowycky, M. C. (1989). Two types of calcium channels coexist in peptide releasing vertebrate nerve terminals. *Neuron* **2**, 1419–1426.

Lindau, M., Stuenkel, E. L. & Nordmann, J. J. (1992). Depolarization, intracellular calcium and exocytosis in single vertebrate nerve endings. *Biophysical Journal* **61**, 19–30.

Lindgren, C. A. & Moore, J. M. (1991). Calcium current in motor nerve endings of the lizard. *Annals of the New York Academy of Sciences* **635**, 58–69.

Llinas, R., Steinberg, I. Z. & Walton, K. (1976). Presynaptic calcium currents and their relation to synaptic transmission: Voltage clamp study in squid giant synapse and theoretical model for the calcium gate. *Proceedings of the National Academy of Sciences of the USA* **73**, 2918–2922.

Moore, C. L. (1971). Specific inhibition of mitochondrial Ca^{2+} transport by ruthenium red. *Biochemical and Biophysical Research Communications* **42**, 298–305.

Nachshen, D. A. (1985). Regulation of cytosolic calcium concentration in presynaptic nerve endings isolated from rat brain. *Journal of Physiology* **363**, 87–101.

Neher, E. (1989). Combined fura-2 and patch clamp measurements in rat peritoneal mast cells. In *Neuromuscular Junction*, ed. Sellin, L. C., Libelius, R. & Thesleff, S., pp. 65–76. Elsevier, New York.

Neher, E. & Augustine, G. J. (1992). Calcium gradients and buffers in bovine chromaffin cells. *Journal of Physiology* **450**, 273–301.

Nicaise, G., Maggio, K., Thirion, S., Horoyan, M. & Keicher, E. (1992). The calcium loading of secretory granules. A possible key event in stimulus-secretion coupling. *Biology of the Cell* **75**, 89–99.

Nicholls, D. G. (1989). Regulation of calcium in isolated nerve terminals (synaptosomes): Relationship to neurotransmitter release. *Annals of the New York Academy of Sciences* **568**, 81–88.

Nordmann, J. J. (1977). Ultrastructural morphometry of the rat neurohypophysis. *Journal of Anatomy* **132**, 213–218.

Nordmann, J. J., Dayanithi, G. & Lemos, J. R. (1987). Isolated neurosecretory nerve endings as a tool for studying the mechanism of stimulus–secretion coupling. *Bioscience Reports* **7**, 411–426.

Nordmann, J. J. & Stuenkel, E. L. (1986). Electrical properties of axons and neurohypophysial nerve terminals and their relationship to secretion in the rat. *Journal of Physiology* **380**, 521–539.

Nordmann, J. J. & Zyzek, E. (1982). Calcium efflux from the rat neurohypophysis. *Journal of Physiology* **325**, 281–299.

Obaid, A. L., Flores, R. & Salzberg, B. M. (1989). Calcium channels that are required for secretion from intact nerve terminals of vertebrates are sensitive to ω-conotoxin and relatively insensitive to dihydropyridines. *Journal of General Physiology* **93**, 715–729.

Ondera, K. (1973). Effect of caffeine on the neuromuscular junction of the frog, and its relation to external calcium concentration. *Japanese Journal of Physiology* **23**, 587–597.

Poulain, D. A. & Wakerley, J. B. (1982). Electrophysiology of hypothalamic magnocellular neurones secreting oxytocin and vasopressin. *Neuroscience* **7**, 773–808.

Pusch, M. & Neher, E. (1988). Rates of diffusional exchange between small cells and a measuring patch pipette. *Pflügers Archiv* **411**, 204–211.

Requena, J. & Mullins, L. J. (1979). Calcium movement in nerve fibres. *Quarterly Reviews of Biophysics* **12**, 371–460.

Stuenkel, E. L. (1990). Effects of membrane depolarization on intracellular calcium in single nerve terminals. *Brain Research* **529**, 96–101.

Stuenkel, E. L. (1993). Regulation of intracellular calcium in isolated secretory nerve endings of the neurohypophysis. *Society for Neuroscience Abstracts* **119**, 1124.

Stuenkel, E. L. & Nordmann, J. J. (1993*a*). Intracellular calcium and vasopressin release of rat isolated neurohypophysial nerve endings. *Journal of Physiology* **468**, 335–355.

Stuenkel, E. L. & Nordmann, J. J. (1993*b*). Sodium-evoked, calcium-independent vasopressin release from rat isolated neurohypophysial nerve endings. *Journal of Physiology* **468**, 357–378.

THAYER, S. A. & MILLER, R. J. (1990). Regulation of the intracellular free calcium concentration in single rat dorsal root ganglion neurones *in vitro*. *Journal of Physiology* **425**, 85–115.

TURNER, T. J., ADAMS, M. E. & DUNLAP, K. (1992). Calcium channels coupled to glutamate release identified by ω-Aga IVA. *Science* **258**, 310–313.

VAN ELDIK, L. J., ZENDEGUI, J. G., MARSHAK, D. R. & WATTERSON, D. M. (1982). Calcium-binding proteins and the molecular basis of calcium action. *International Review of Cytology* **77**, 1–61.

WILSON, D. F. (1973). Effects of caffeine on neuromuscular transmission in the rat. *American Journal of Physiology* **225**, 862–865.

ZHOU, Z. & NEHER, E. (1993). Mobile and immobile calcium buffers in bovine adrenal chromaffin cells. *Journal of Physiology* **469**, 245–273.

Acknowledgements

I thank I. M. Cooke and J. J. Nordmann for valuable comments on the manuscript. This work was supported by NSF grant 9111092.

Received 25 November 1993; accepted 6 May 1994.